

## Peer Review File

---

Multiplexed volumetric CLEM enabled by scFvs provides new insights into the cytology of cerebellar cortex



**Open Access** This file is licensed under a Creative Commons Attribution 4.0

International License, which permits use, sharing, adaptation, distribution and reproduction in any medium or format, as long as you give appropriate credit to

the original author(s) and the source, provide a link to the Creative Commons license, and indicate if changes were made. In the cases where the authors are anonymous, such as is the case for the reports of anonymous peer reviewers, author attribution should be to 'Anonymous Referee' followed by a clear attribution to the source work. The images or other third party material in this file are included in the article's Creative Commons license, unless indicated otherwise in a credit line to the material. If material is not included in the article's Creative Commons license and your intended use is not permitted by statutory regulation or exceeds the permitted use, you will need to obtain permission directly from the copyright holder. To view a copy of this license, visit <http://creativecommons.org/licenses/by/4.0/>.

## REVIEWER COMMENTS

Reviewer #1 (Remarks to the Author):

The authors developed eight smaller single-chain variable fragments (scFvs) based on eight well-characterized mAbs and conjugated them with various fluorescent dyes. This idea is great for volume correlative light and electron microscopy. The authors reported that each scFv proved effective as a detergent-free immunofluorescent probe. The approach was believed to be promising for routine linking of molecular information to connectomic information from the same material since the quality of data from the volumetric fluorescent and electron microscopy is good. However, some critical aspects of the experimental design need to be addressed, and additional experiments are required to draw conclusive findings.

1. One concern in this study is to choose Triton X-100 as a detergent for comparison. While Triton X-100 is commonly used to aid antibody penetration in light microscopy, it is not widely used for EM or immuno-EM studies. For EM studies, saponin is one of organic solvents which dissolve lipids from cell membranes making them permeable to antibodies. Furthermore, organic solvents can be used to fix and permeabilize cells at the same time by coagulating proteins. Saponin interacts with membrane cholesterol, selectively removing it and leaving holes in the membrane. Most researchers in the EM field choose low concentration of saponin to balance the antibody penetration and excellent membrane morphology in their immuno-EM experiments. Majority of their immuno-EM images showed great morphology of membrane at the ultrastructural level with the use of saponin. In some immuno-EM studies, Triton X-100 has been used. But those studies don't care the cell membrane, most of them were interested in some subcellular organelles.

2. Another point of concern is the lack of clarity on how the antibodies penetrate the cell through the cell membrane in detergent-free immunofluorescence labeling. A more thorough investigation and explanation of this process are needed to provide a comprehensive understanding of the technique's efficacy.

3. The animals were perfused with the fixative (4% paraformaldehyde + 0.1% glutaraldehyde). The low concentration of glutaraldehyde (0.1%) may not be sufficient to adequately preserve the lipids in the cell membrane. However, for detergent-free immunofluorescence labeling, scFv probes or nanobody probes were incubated for 3 days (50  $\mu\text{m}$ ) or 7 days (120  $\mu\text{m}$ ). This could potentially affect the ultrastructural morphology.

4. This study lack of novelty. The use of scFv has been well-established over the years, making it a solid foundation for the volume CLEM study. However, the choice of detergent-free immunofluorescence labeling raises questions about its suitability. Considering alternative approaches, such as utilizing low concentrations of saponin, might offer a more effective option for preserving membrane morphology during immuno-EM experiments.

5. The choice of 0.3% Triton X-100 to demonstrate detergent issues in EM seems excessive. Most EM studies recommend not exceeding 0.1% Triton X-100, making it unnecessary to use a higher concentration for this purpose.

Reviewer #2 (Remarks to the Author):

This is a technology development manuscript describing the generation and implementation of an assortment of single chain antibody-based probes (scFvs) against different brain proteins to label tissue for correlative fluorescence/volumetric electron microscopy. The key advance is the nature of the labeling probes, which can diffuse deep into fixed brain tissue and penetrate cells without the need for detergent permeabilization. The authors do nice side-by-side comparisons with whole IgG antibodies to highlight this. Detergent-free labeling thus allows processing for ultrastructural analysis

by EM, with excellent membrane preservation. Furthermore, the scFv labeling reagents can be easily labeled with different fluorescent dyes allowing the authors to visualize numerous (here they show 6) different labels in the same sample using spectral unmixing confocal microscopy. Serial section EM images of the same samples were then reconstructed and aligned with the fluorescence images to achieve correlated fluorescence/ultrastructure. Overall the data were compelling, with many beautiful examples of correlated fluorescence localization with 3D ultrastructure, nicely demonstrating the power of the technique. While the manuscript primarily focuses on tool development and offers little in the way of novel biological insight, I feel the potential future impact of the technique (i.e. ability to assign neural identities to volumetric connectomics EM datasets, ultrastructural localization of channels, receptors, etc.) will have broad appeal. There are several specific points that deserve attention:

-Nowhere in the manuscript do the authors validate their labeling reagents in a knockout background. In many cases the labeling pattern is distinct, consistent with previously published work and the localization of the signal makes sense with the correlated ultrastructure (i.e. vGLUT labels presynaptic terminals), but in some cases it is more ambiguous. For example, in Fig. S2a,e the authors argue that the CB and PV scFvs label more of the target proteins in the cell nucleus, is this real signal or are these probes picking up something non-specific in the nucleus that the IgG does not?

-While many of the images are quite striking, overall the manuscript lacked any sort of quantitative analysis. Just as one example, in Fig. 1, showing a simple pixel correlation scatter plot comparing the YFP and GFP-scFv signal would give readers a better idea of how evenly the scFv is penetrating cells to label YFP.

-p. 9 ".....immunofluorescence patterns that were similar to or in some cases stronger than their parental mAbs in Crus 1 of the cerebellar cortex (Figure 2 a; Sup. Figure 2; Sup. Figure 3). In many cases the comparisons between mAb and scFv is not entirely fair since the mAb is labeled in the 488/green channel (in which brain tissue notoriously has more autofluorescence) and the scFv in the red channel e.g. NPY signal in Sup. 2b,d; PSD95 in Sup. 2f. Is the labeling really that much cleaner or is the background signal in the green channel making the mAb appear worse than it is?

-p. 9 ".....found that the anti-calbindin scFv penetrated to a depth of ~150  $\mu\text{m}$  in a 300- $\mu\text{m}$  tissue slice". So the probe labeled throughout the entire slice?

1 **REVIEWER COMMENTS**

2

3 **Reviewer #1 (Remarks to the Author):**

4 *The authors developed eight smaller single-chain variable fragments (scFvs) based on eight*  
5 *well-characterized mAbs and conjugated them with various fluorescent dyes. This idea is great*  
6 *for volume correlative light and electron microscopy. The authors reported that each scFv*  
7 *proved effective as a detergent-free immunofluorescent probe. The approach was believed to*  
8 *be promising for routine linking of molecular information to connectomic information from the*  
9 *same material since the quality of data from the volumetric fluorescent and electron microscopy*  
10 *is good. However, some critical aspects of the experimental design need to be addressed, and*  
11 *additional experiments are required to draw conclusive findings.*

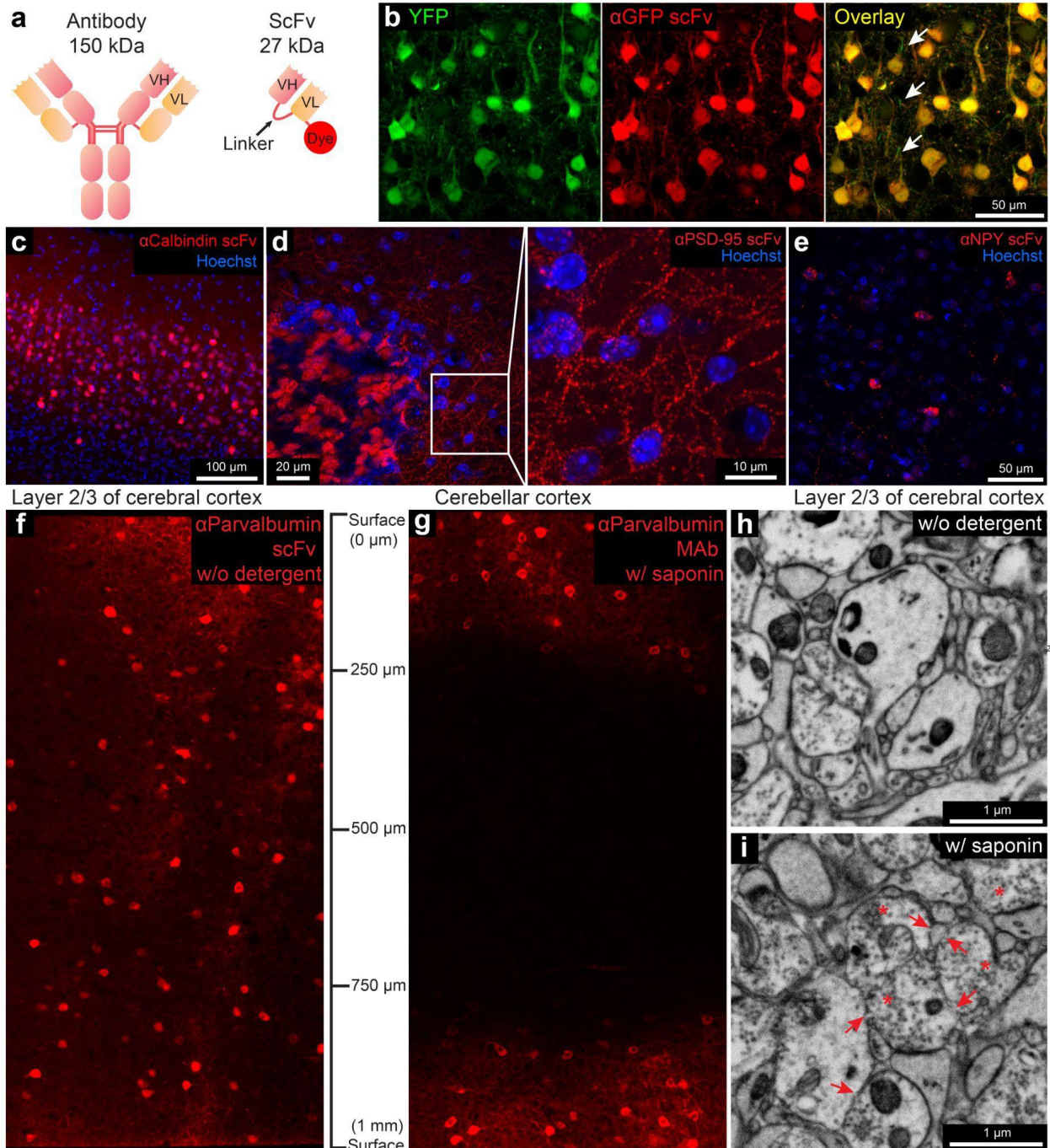
12

13 *1. One concern in this study is to choose Triton X-100 as a detergent for comparison. While*  
14 *Triton X-100 is commonly used to aid antibody penetration in light microscopy, it is not widely*  
15 *used for EM or immuno-EM studies. For EM studies, saponin is one of organic solvents which*  
16 *dissolve lipids from cell membranes making them permeable to antibodies. Furthermore,*  
17 *organic solvents can be used to fix and permeabilize cells at the same time by coagulating*  
18 *proteins. Saponin interacts with membrane cholesterol, selectively removing it and leaving holes*  
19 *in the membrane. Most researchers in the EM field choose low concentration of saponin to*  
20 *balance the antibody penetration and excellent membrane morphology in their immuno-EM*  
21 *experiments. Majority of their immuno-EM images showed great morphology of membrane at*  
22 *the ultrastructural level with the use of saponin. In some immuno-EM studies, Triton X-100 has*  
23 *been used. But those studies don't care the cell membrane, most of them were interested in*  
24 *some subcellular organelles.*

25 We thank the reviewer for pointing out the important fact that saponin is a far better  
26 detergent for electron microscopy ultrastructural studies than Triton X-100. In response to this  
27 suggestion, we did a new series of experiments analyzing twenty-two tissue blocks at various  
28 saponin concentrations, sample thicknesses, and durations of antibody incubation. Moreover,  
29 directly conjugated mAbs have become available, so we moved the results related to the  
30 penetration tests with secondary antibody labeling (original Figure 1 d and e) to Supplementary  
31 Figure 3 b and c). The new results are now presented in new Figure 1 panels f-i, new  
32 Supplementary Figure 4 (plus additional new Supplementary Figure 5 that we will describe  
33 below in point 4). The key result is that saponin at 0.05% concentration does not allow  
34 fluorescently labeled monoclonal antibodies to penetrate into the middle 500  $\mu\text{m}$  of a 1-mm  
35 block even after a 1-week incubation with the labeled antibody (Figure 1 g; Supplementary  
36 Figure 4). In contrast, the fluorescently labeled scFv penetrated throughout a block in the  
37 absence of detergent (Figure 1 f; Supplementary Figure 4). In different experiments, we did  
38 examine if higher concentrations of saponin could aid in deeper penetration (see new  
39 Supplementary Figure 5) but for our purposes, even saponin at 0.05% was problematic. The  
40 reason was that we found small breaks in the plasma membranes of neuronal processes  
41 (arrows, Fig 1 i) that were not present in samples not treated with detergent (Fig 1 h). While  
42 these ultrastructural breaks are small and, for many kinds of studies, would be of no  
43 consequence, for connectomics they are serious. This seriousness is related to the requirement  
44 for automatic algorithms to segment each nerve cell process. When two adjacent objects have a

45 continuity between them, this is often interpreted by the algorithms erroneously as the same  
46 object. Such merge errors are far more difficult to find and correct than split errors, so avoiding  
47 them at all costs is necessary (Shapson-Coe et al. 2021; Januszewski et al. 2018). With newer  
48 techniques like multicolor 2-photon microscopy (Mahou et al. 2012; Blanc et al. 2023; Pudavar  
49 et al. 2024), lightsheet microscopy in uncleared tissue (Schmid et al. 2013), and confocal done  
50 with clearing approaches compatible with electron microscopy (Furuta et al. 2022), we think  
51 having fluorescent scFv penetration hundreds of microns into tissue blocks will be of great use  
52 in CLEM studies. We have modified the text to make these points clearer (line 150).

53



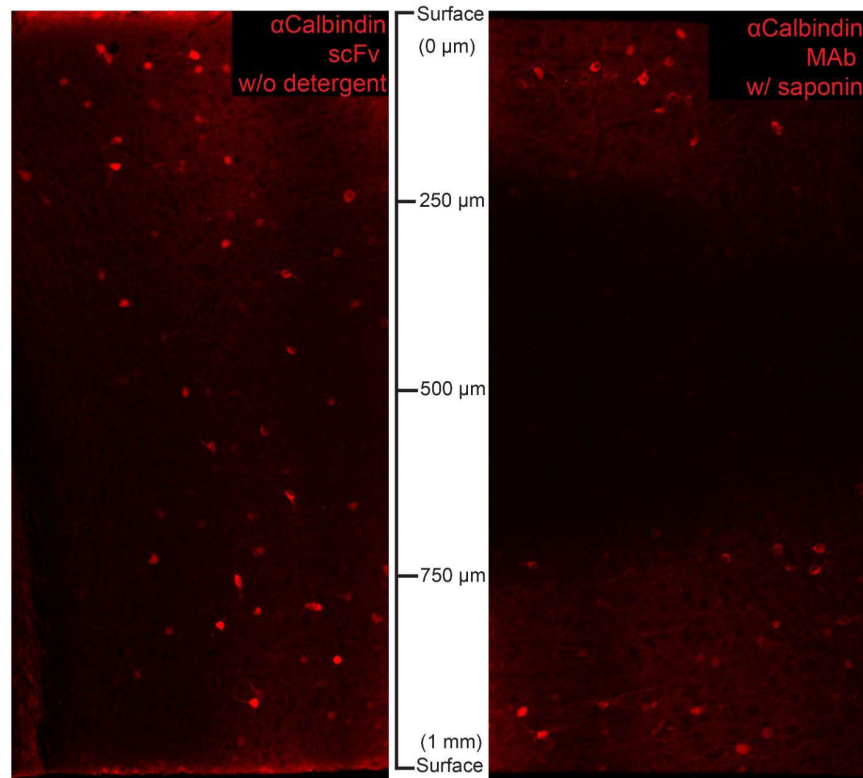
54

55 **Figure 1. Fluorescent scFv probes label brain tissues without detergents to preserve electron**  
 56 **microscopy ultrastructure.**

57 **a**, Schematic representations of a full-length IgG antibody and an scFv probe with a conjugated  
 58 fluorescent dye. **b**, Confocal images from the cerebral cortex of a YFP-H mouse labeled using a GFP-  
 59 specific scFv probe conjugated with the red dye 5-TAMRA. Arrows show thinner neuronal processes,  
 60 perhaps myelinated, that are not labeled by scFv. **c**, Layer 2/3 of the cerebral cortex labeled with a  
 61 calbindin-specific scFv probe. **d**, Cerebellum cortex of Crus 1 labeled with the PSD-95 specific scFv. Right  
 62 panel is the enlarged boxed inset from left. **e**, Cerebral cortex labeled with the NPY-specific scFv. **f** and **g**,  
 63 Tissue penetration comparison of a parvalbumin-specific scFv without detergent and its parental



64 mAbs directly conjugated with fluorophores with 0.05% saponin on 1-mm cerebral cortex tissue sections  
65 with a 7-day incubation. **h** and **i**, Comparison of ultrastructure from samples incubated 7 days without  
66 detergent and with 0.05% saponin. Arrows indicate membrane breaks. Asterisks indicate abnormal  
67 appearing vesicle-filled axonal terminals.  
68



69  
70  
71 **Sup. Figure 4. Penetration of anti-calbindin scFv into 1-mm tissue sample.**

72 Tissue penetration depth comparison of a calbindin-specific scFv without detergent and its parental mAbs  
73 directly conjugated with fluorophores with 0.05% saponin on 1-mm cerebral cortex tissue sections with a  
74 7-day incubation.  
75

76 *2. Another point of concern is the lack of clarity on how the antibodies penetrate the cell through*  
77 *the cell membrane in detergent-free immunofluorescence labeling. A more thorough*  
78 *investigation and explanation of this process are needed to provide a comprehensive*  
79 *understanding of the technique's efficacy.*

80 We agree with the reviewer on the importance of investigating how scFvs penetrate the  
81 cell membrane in the absence of detergent. We are interested in determining the mechanism as  
82 well. We think there are at least two possible mechanisms:

83 First, because all the immunolabeling experiments in this study were performed on brain  
84 tissue samples from animals perfused and fixed with 4% formaldehyde (prepared fresh from  
85 paraformaldehyde) + 0.1% glutaraldehyde in PBS, the cell membrane penetration by scFvs may  
86 be simply explained by the fact that formaldehyde and glutaraldehyde permeate the lipid bilayer.  
87 formaldehyde and glutaraldehyde are commonly used as chemical fixatives by crosslinking  
88 amino groups of proteins (Fischer et al. 2008). It has been known that formaldehyde also

89 dissolves lipids (Fox et al. 1985; Kiernan 2000; Thavarajah et al. 2012). A recent study using  
90 surface plasmon resonance (SPR) (Cheng et al. 2019) showed that fixation with formaldehyde  
91 perturbed the integrity of membranes ( $10 \pm 5\%$  mass loss), and they showed increased  
92 permeability of sucrose. In another recent study using atomic force microscopy (Ichikawa et al.  
93 2022), both formaldehyde and glutaraldehyde were shown to increase the size of nanoscopic  
94 protrusions on cell membranes. These protrusions were generated by membrane protein  
95 aggregates induced by crosslinking via formaldehyde or glutaraldehyde. The aggregated  
96 membrane proteins may create gaps between them and their nearby lipids providing a  
97 permeability pore. Additionally, two extracellular space-preserving fixation methods employing  
98 formaldehyde and glutaraldehyde (Fulton and Briggman 2021; Lu et al. 2023) showed that full-  
99 length antibodies can penetrate cell membranes albeit with lower diffusivity than scFvs,  
100 supporting the idea that the formaldehyde plus glutaraldehyde treated membranes do have  
101 gaps caused by the fixation.

102 We have tested this idea as well by using scFv immunolabeling on HEK293T cells  
103 cultured as a single layer on a petri dish with a coverglass bottom. HEK293T cells allowed us to  
104 avoid the issue of cut/fragmented cells in tissue sections where scFv could penetrate into cells  
105 via a cut surface rather than through a membrane. After transfecting the HEK293T cells with a  
106 plasmid encoding calbindin, we fixed the cells with the same fixative (4% formaldehyde + 0.1%  
107 glutaraldehyde in PBS) for 15 min and then washed with PBS. Overnight immunolabeling of the  
108 anti-calbindin scFv was then performed without or with 0.1% Triton-X. The results showed that  
109 in both conditions (without or with 0.1% Triton-X), the scFv can penetrate and label its  
110 intracellular target (we have added a new Supplementary Figure 7 a, b to show this data). This  
111 result provides evidence consistent with the idea that the cell membranes fixed with 4%  
112 formaldehyde + 0.1% glutaraldehyde allow scFvs to penetrate into intracellular spaces.  
113 Additionally, we also tested a 1-hour immunolabeling protocol using scFvs and full-size mAbs  
114 directed to transfected calbindin in COS-1 cells both without and with detergent  
115 permeabilization. Similarly, we found that the scFvs were able to penetrate COS-1 cells and  
116 label intracellular targets. However, the mAb was unable to penetrate at least at 1 hour (see  
117 new Supplementary Figure 8). In another experiment we did find that an overnight incubation  
118 with a mAb did label fixed cells that were not permeabilized with detergent. From all of these  
119 experiments we infer that due to their small size the scFvs are better to penetrate fixed cells  
120 than larger immunoprobos. We have modified the text to make these points clearer (line 169).

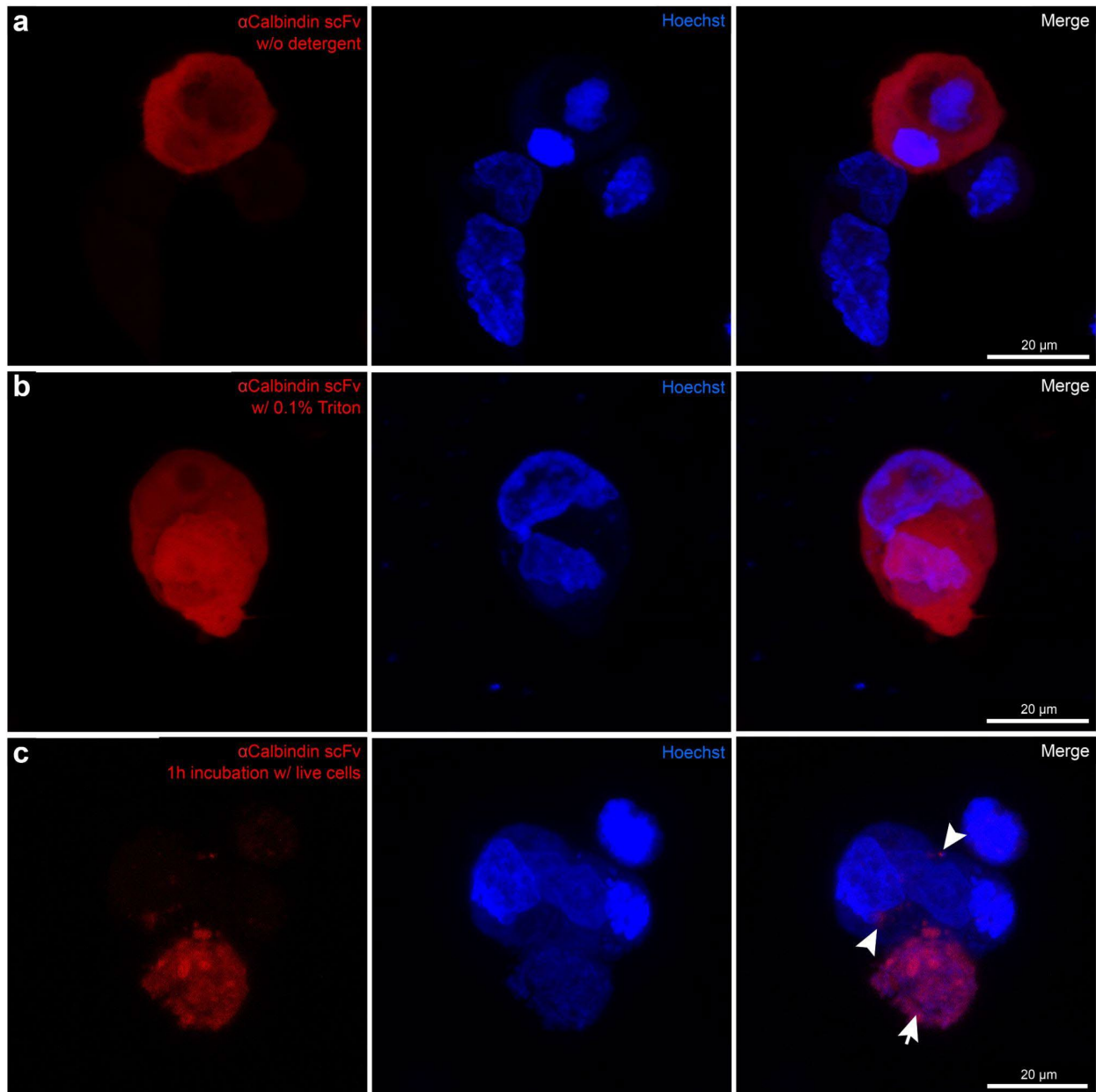
121 It is also possible that scFvs by virtue of their small size could permeate unfixed lipid  
122 bilayers. Indeed (Li et al. 2016) showed that anti-pTau nanobodies when injected into the blood  
123 of live mice could cross the blood-brain barrier and also cross neuronal cell membranes to label  
124 intracellular pTau. In (Bernard et al. 2016), after transgenically inducing expression of an anti-  
125 Otx2 scFv to express in cells of the choroid plexus cells, scFv in the CSF can cross the blood-  
126 brain barrier and neutralize Otx2 in the cortex, perhaps via transcytosis. In (Thiel et al. 2002),  
127 scFvs were shown to be able to pass through live cornea with an intact epithelium. (Im, Chung,  
128 and Jang 2017) showed that scFvs can enter live, unfixed culture cells.

129 Based on these results, we were motivated to see if the scFvs we generated could cross  
130 into living cells. We attempted to immunolabel the transfected HEK293T cell for calbindin with  
131 the anti-calbindin scFv using live HEK293T cells. We found that after a one-hour incubation, the  
132 scFv could penetrate cells (Supplementary Figure 7 c, arrow). However, unlike the penetration  
133 of fixed cells described above, the labeling was more punctate. This labeling was most likely



134 explained by endocytosis as has been previously seen for extracellular dye molecules (see for  
135 example, (Tsuriei et al. 2015)). We have added a Supplementary Figure 7 c to show this result.  
136 Consistent with this, it has been documented that both nanobodies and scFvs can be  
137 internalized into cells via endocytosis (de Beer and Giepmans 2020; Wittrup et al. 2009; Alric et  
138 al. 2018; Kim et al. 2020). We have modified the text to make this point clearer (line 176). This  
139 is a potentially important route of entry because it provides an option to achieve immunolabeling  
140 of larger tissue samples, such as a whole mouse brain, by introducing these small immuno-  
141 probes in live animals.

142



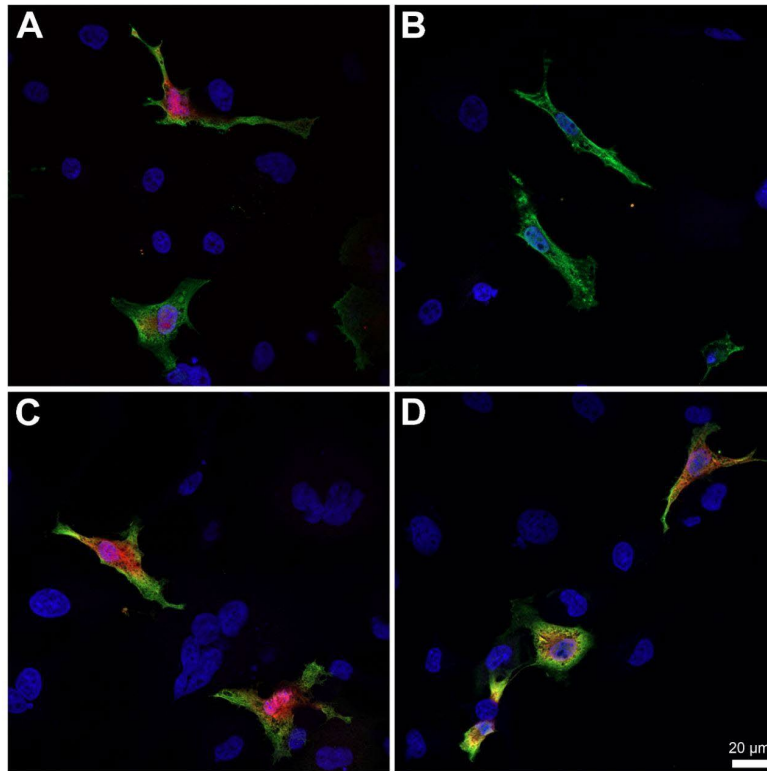
143

144

145

Sup. Figure 7. Penetration of anti-calbindin scFv into fixed HEK cells or live cells.

146 Immunofluorescence immunocytochemistry on transiently transfected cells. HEK cells were transfected  
147 with a plasmid encoding Flag-tagged human calbindin. **a**, Chemically fixed cells were labeled overnight  
148 with Alexa594 anti-calbindin L109/57 scFv in the absence of detergent. **b**, Chemically fixed cells were  
149 labeled overnight with Alexa594 anti-calbindin L109/57 scFv with 0.1% Triton-X. **c**, Live cells were labeled  
150 with Alexa594 anti-calbindin L109/57 scFv. The arrow indicates the cell that has intracellular scFv  
151 labeling. Arrowheads indicate puncta labeling in some cells.  
152



153  
154  
155 **Sup. Figure 8. Penetration of anti-calbindin scFv into fixed COS-1 cells.**

156 Immunofluorescence immunocytochemistry on transiently transfected cells. COS-1 cells were transfected  
157 with a plasmid encoding Flag-tagged human calbindin. Cells in panels A and B were labeled for 1 hour  
158 after fixation and prior to detergent permeabilization with (A) Alexa594 anti-calbindin L109/57 scFv or (B)  
159 anti-calbindin mouse mAb L109/39 (scFv and mAb labeling in red). After permeabilization, cells were  
160 labeled with rabbit anti-Flag (green) to detect calbindin, and Hoechst nuclear dye (blue). For cells in  
161 panels C and D all immunolabeling was performed after fixation and detergent permeabilization with (C)  
162 Alexa594 anti-calbindin L109/57 scFv or (D) anti-calbindin mouse mAb L109/39 (scFv and mAb labeling  
163 in red). Cells were simultaneously labeled with rabbit anti-Flag (green), and Hoechst (blue). Cells in all  
164 panels were imaged at the same exposure.  
165

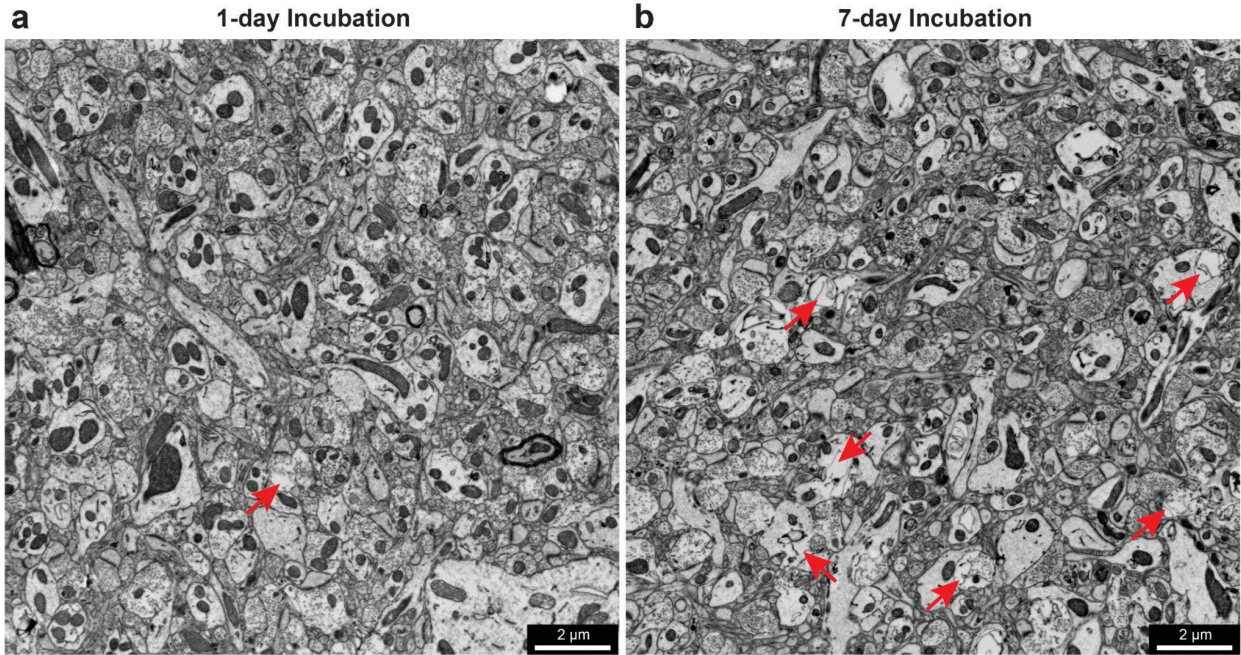
166 *3. The animals were perfused with the fixative (4% paraformaldehyde + 0.1% glutaraldehyde).*  
167 *The low concentration of glutaraldehyde (0.1%) may not be sufficient to adequately preserve the*  
168 *lipids in the cell membrane. However, for detergent-free immunofluorescence labeling, scFv*  
169 *probes or nanobody probes were incubated for 3 days (50 μm) or 7 days (120 μm). This could*  
170 *potentially affect the ultrastructural morphology.*

171 We agree this is a reasonable concern that the use of 0.1% glutaraldehyde does not  
172 sufficiently preserve lipids in the cell membrane, which may cause the ultrastructure to  
173 deteriorate when tissue samples are incubated with immuno-probes for prolonged periods like

174 three or seven days. We were aware of this potential problem. The reasons we used 0.1%  
175 glutaraldehyde instead of a higher concentration was: first, glutaraldehyde is a harsher fixative  
176 which may modify epitopes on target proteins (Fischer et al. 2008), preventing immuno-probe  
177 labeling; Second, glutaraldehyde has higher autofluorescence than formaldehyde (Fischer et al.  
178 2008), which causes high background in fluorescence microscopy. Because we only used 0.1%  
179 glutaraldehyde, we always postfixed the perfused brain for many hours (overnight). To prevent  
180 reversal of the formaldehyde fixation (Fischer et al. 2008) the brain samples were then sliced in  
181 ice-cold fixative (4% formaldehyde + 0.1% glutaraldehyde) and stored in the same fixative at  
182 4 °C. The only exception to this protocol was our work with the neuropeptide NPY, which we, as  
183 others, have found to be difficult to label if the fixation is too extensive. In this case, we stored  
184 the slices in PBS at 4 °C. We also performed all the incubations, including the washing steps, at  
185 4 °C to prevent ultrastructural degradation. In the manuscript, in Supplementary Figure 21, we  
186 examined the ultrastructure of a 2 mm, 2 mm, 120- $\mu$ m thick cerebellum tissue sample incubated  
187 with scFv probes for seven days after light fixation (described above). As shown in the figure,  
188 ultrastructure at four locations across the cerebellar cortex layers including regions that are near  
189 the center of the block, is preserved well. After careful examination of the images during the  
190 revision process, we have noticed some abnormalities. In the superficial layer (the molecular  
191 layer) of the cerebellar cortex, which is mainly composed of neuronal processes and close to  
192 the surface of the block, we did observe some artifacts (new arrows in Supplementary Figure  
193 21). We are unsure whether these artifacts are explained by mechanical or chemical or thermal  
194 factors that are different at the surface vs. the interior of the block. We have also modified the  
195 manuscript (line 217) to make readers aware of this issue. If reviewers are interested in  
196 examining the ultrastructure directly, we encourage reviewers to visit the Neuroglancer link of  
197 our vCLEM dataset at [Neuroglancer LINK](#).

198 In addition, in a new set of experiments we performed for the revision that we will  
199 discuss in detail below in point 4, we showed that instead of 3-day or 7-day incubations, the  
200 anti-calbindin scFv can penetrate to the center of a 300- $\mu$ m vibratome section with incubation of  
201 only one day. We found fewer tissue artifacts in the ultrastructure of 1-day incubated samples  
202 than the 7-day samples (see an example in new Supplementary Figure 6, arrows indicating  
203 artifacts). We have modified the text to make this point clearer (line 166). So, we conclude that,  
204 at least for some scFvs, 1-day incubations are sufficient.

205

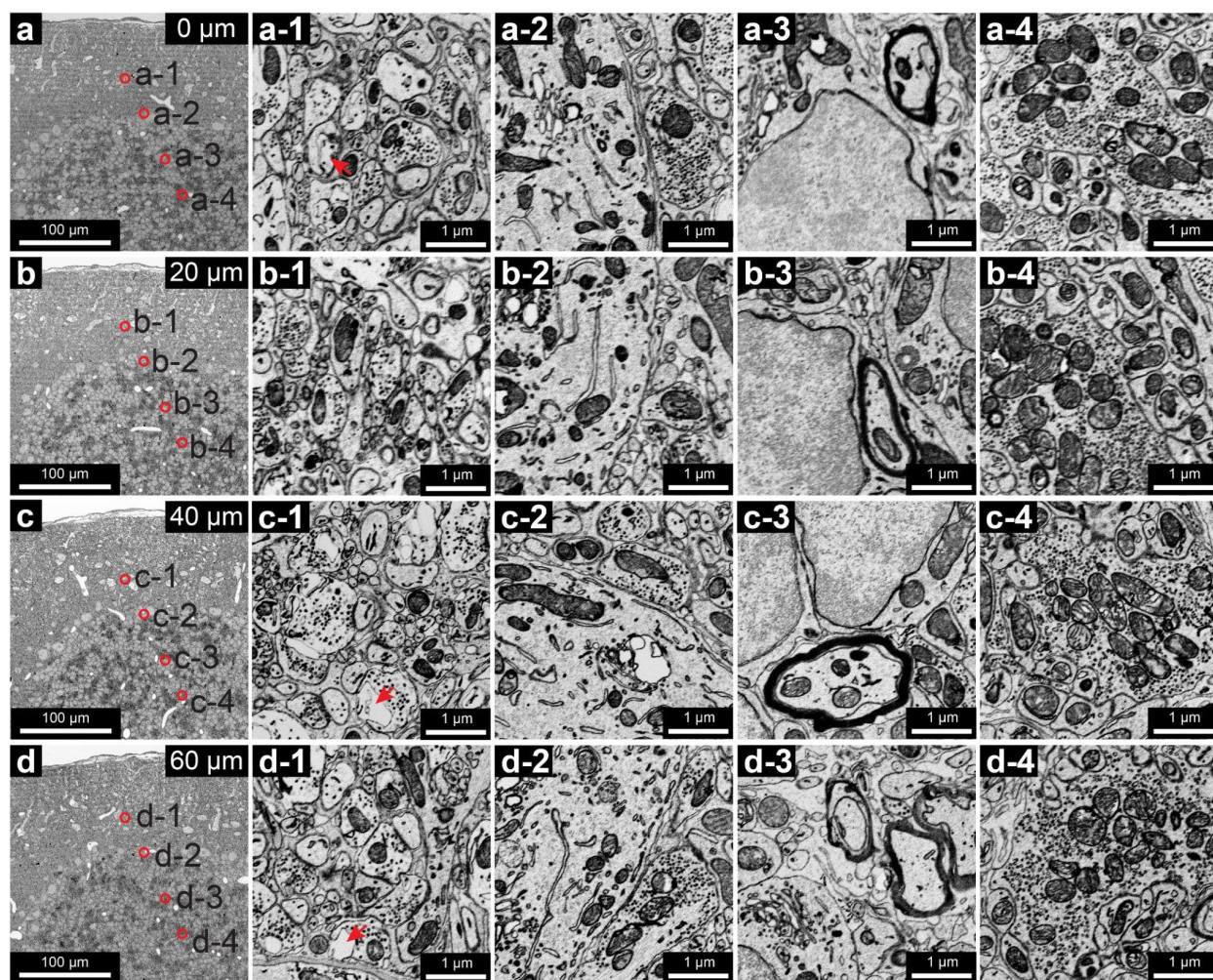


206  
207  
208

**Sup. Figure 6. Ultrastructure comparison between samples incubated for one day or seven days.**

209 Ultrastructure of locations close to the surfaces of 300- $\mu\text{m}$  cerebral cortex sections immunolabeled for  
210 one day (a) or seven days (b). Arrows indicate artifacts.  
211





212

213 **Sup. Figure 21. Well-preserved ultrastructure from the surface (a) to the middle (d) of the 120- $\mu$ m**  
 214 **section.**

215 Panel 1-4 in a-d show the ultrastructure at the locations labeled by the red circles in the right panels.  
 216 Arrows indicate the artifacts potentially caused by prolonged incubation with scFvs for immunolabeling.  
 217

218 *4. This study lack of novelty. The use of scFv has been well-established over the years, making*  
 219 *it a solid foundation for the volume CLEM study. However, the choice of detergent-free*  
 220 *immunofluorescence labeling raises questions about its suitability. Considering alternative*  
 221 *approaches, such as utilizing low concentrations of saponin, might offer a more effective option*  
 222 *for preserving membrane morphology during immuno-EM experiments.*

223 We agree with the reviewer that the use of scFvs is well-established (Bird et al. 1988;  
 224 Huston et al. 1988; Monnier, Vigouroux, and Tassew 2013; Ahmad et al. 2012). The use of  
 225 scFvs as immuno-probes for CLEM has been raised in a number of papers in discussion (de  
 226 Beer and Giepmans 2020; Franek et al. 2024) but, to the best of our knowledge, this is the first  
 227 actual demonstration of scFvs in volumetric CLEM.

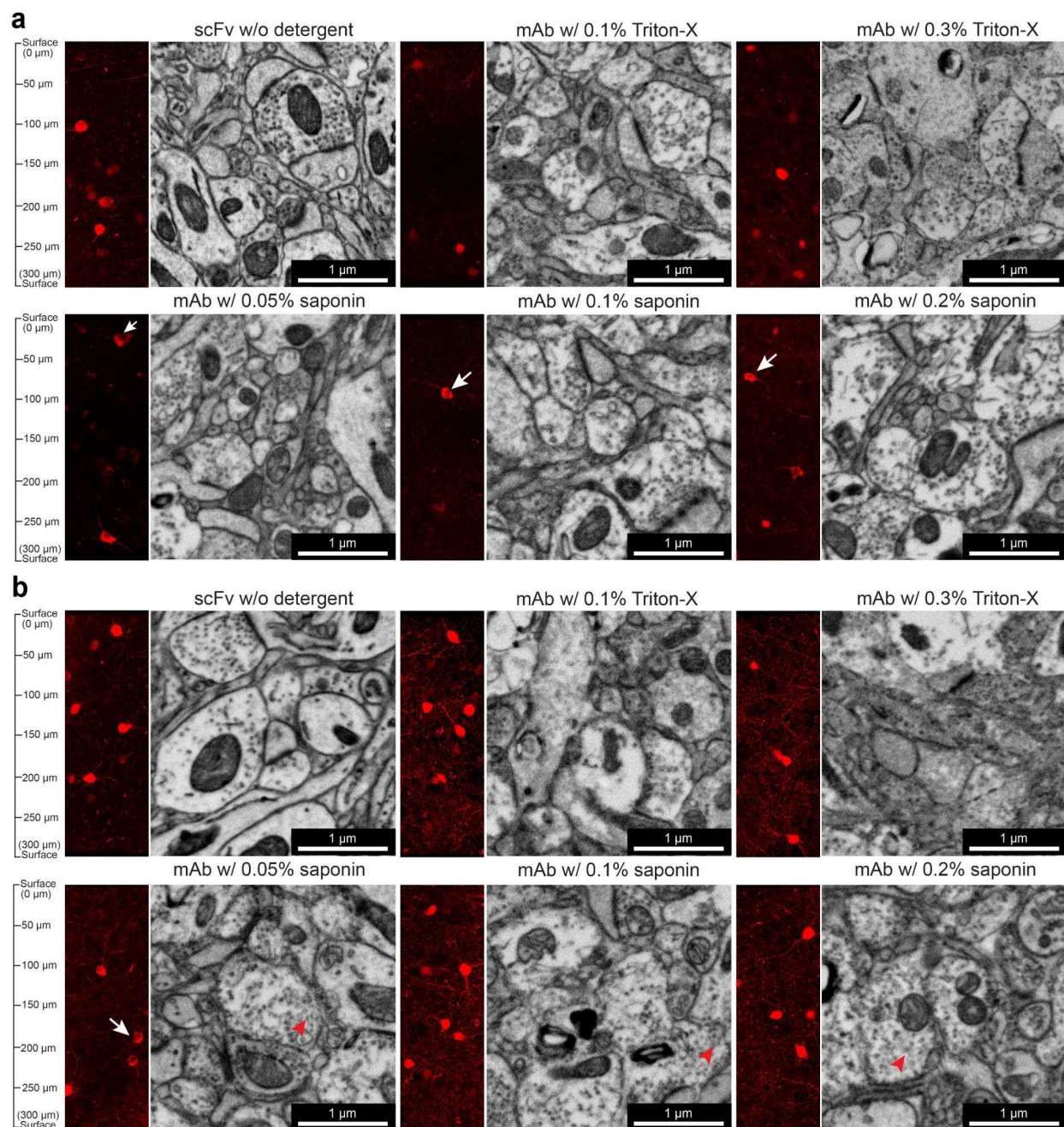
228 We agree with the reviewer that when performing volumetric CLEM, alternative  
 229 immunolabeling approaches other than those that employ scFvs should be considered, such as

230 fluorescently tagged primary IgG antibodies with saponin permeabilization. Therefore, in new  
231 experiments we compared detergent-free immunolabeling with scFv and Triton-X or saponin-  
232 enabled immunolabeling with a dye-directly conjugated monoclonal antibody (mAb) at various  
233 detergent concentrations (0.1% and 0.3% Triton-X; 0.05%, 0.1%, and 0.2% saponin) and with  
234 two different incubation times (1 day and 7 days). The experiments were performed on 300- $\mu$ m  
235 cerebral cortex tissue blocks with an anti-calbindin L109/57 scFv and a dye-directly conjugated  
236 anti-calbindin L109/57 mAb. The epitope binding site of the mAb and the scFv were the same.  
237 As shown in new Supplementary Figure 5 a, after 1 day of incubation, only the scFv and the  
238 mAb with 0.3% Triton-X penetrated to the middle (i.e., 150  $\mu$ m) of the section. The other  
239 experimental conditions showed various degrees of penetration: 0.1% Triton-X,  $\sim$ 50  $\mu$ m; 0.05%  
240 saponin,  $\sim$ 30  $\mu$ m; 0.1% saponin,  $\sim$ 80  $\mu$ m; 0.2% saponin,  $\sim$ 100  $\mu$ m. In all cases with saponin  
241 permeabilization, there was a lack of labeling in the cell nuclei (indicated by arrows). When we  
242 examined the ultrastructure of these labeled samples, the samples treated with detergent-free  
243 scFv labeling showed the best quality. The sample treated with 0.05% saponin showed good-  
244 quality EM ultrastructure. All the other samples showed compromised EM ultrastructure, the  
245 severity of which increased with the increase of detergent concentration. The membrane breaks  
246 in these samples would make automatic segmentation for connectomics challenging, as stated  
247 above in our answer to point 1. Although the sample treated with 0.05% saponin for one day  
248 showed no obvious ultrastructural artifacts, the mAb penetration was far shallower than the scFv  
249 ( $\sim$ 30  $\mu$ m vs. 150  $\mu$ m) making volumetric CLEM on the samples larger than the penetration depth  
250 difficult.

251 As shown in new Supplementary Figure 5 b, after 7 days of incubation, scFvs without  
252 detergent and mAb with various concentrations of Triton-X or saponin can penetrate the middle  
253 of the 300- $\mu$ m. However, we still observed in the case of 0.05% saponin a lack of labeling in the  
254 cell nuclei (indicated by arrows). Again, when examining the ultrastructure of these labeled  
255 samples, the sample treated with detergent-free scFv labeling showed the best quality and is  
256 similar to the one-day sample (which we have also mentioned in our answer to reviewer's point  
257 3). All the other samples showed compromised EM ultrastructure, which was much worse when  
258 compared with the 1-day samples. Even the 0.05% saponin now showed membrane breaks.  
259 We also noticed after 7-day saponin incubation a new artifact: the vesicle-filled axonal profiles in  
260 samples treated with saponin for seven days showed a granular texture (indicated by  
261 arrowheads in Supplementary Figure 5 b). We think the protein-coagulating function of saponin,  
262 as the reviewer stated previously, may be the cause. These granules could pose challenges  
263 when synaptic vesicles need to be automatically detected and analyzed (as we did in the later  
264 part of this paper) for connectomic studies.

265 In addition, as we have mentioned in our answer to point 1, scFvs can penetrate 1-mm  
266 tissue blocks while saponin at 0.05% concentration only allows mAbs to penetrate into 250  $\mu$ m  
267 after a seven-day incubation (Figure 1 g; new Supplementary Figure 4). These new results  
268 suggest that if a researcher wants to do a small-scale volumetric CLEM on a smaller tissue  
269 sample (such as several  $\mu$ m to 50- $\mu$ m), directly dye-conjugated primary antibodies with a low  
270 concentration (0.05%) of saponin with a shorter incubation (one day) may be an option.  
271 However, should a researcher need to conduct large-scale volumetric CLEM on larger tissue  
272 samples ( $\sim$ 1 mm in thickness), using scFvs for detergent-free immunolabeling is more  
273 advantageous. Large-scale volumetric CLEM is especially important for connectomics because  
274 a smaller volume is very likely to have fragmented cells/processes that prevent the mapping of  
275 the neural circuits. We have modified the text to make these points clearer (line 150; line 162).





277  
278  
279  
280

**Sup. Figure 5. Tissue penetration depth comparison of scFvs in the absence of detergent and fluorophore-conjugated mAbs with the treatments of various concentrations of detergents.**

281 300- $\mu\text{m}$  cerebral cortex sections were immunolabeled for one day (a) or seven days (b) with a calbindin-  
282 specific scFv conjugated with 5-TAMRA in the absence of detergent or with the scFv's parental mAb  
283 conjugated with FL550 in the presence of 0.1%, 0.3% Triton-X, or 0.05%, 0.1%, 0.2% saponin. Arrows  
284 indicate unlabeled cell nuclei. Arrowheads indicate granular textures associated with the treatment of  
285 saponin.

286  
287



288 *5. The choice of 0.3% Triton X-100 to demonstrate detergent issues in EM seems excessive.*  
289 *Most EM studies recommend not exceeding 0.1% Triton X-100, making it unnecessary to use a*  
290 *higher concentration for this purpose.*

291           We agree with the reviewer that choosing 0.3% Triton X-100 is excessive to  
292 demonstrate the detergent's issue on EM ultrastructure. We have changed Figure 1 h and i so  
293 the comparison is with a sample treated with 0.05% saponin.

294

295

296

297

298

299

300

301

302

303

304

305

306

307

308

309

310

311

312

313

314

315

316

317

318

319 **Reviewer #2 (Remarks to the Author):**

320 *This is a technology development manuscript describing the generation and implementation of*  
321 *an assortment of single chain antibody-based probes (scFvs) against different brain proteins to*  
322 *label tissue for correlative fluorescence/volumetric electron microscopy. The key advance is the*  
323 *nature of the labeling probes, which can diffuse deep into fixed brain tissue and penetrate cells*  
324 *without the need for detergent permeabilization. The authors do nice side-by-side comparisons*  
325 *with whole IgG antibodies to highlight this. Detergent-free labeling thus allows processing for*  
326 *ultrastructural analysis by EM, with excellent membrane preservation. Furthermore, the scFv*  
327 *labeling reagents can be easily labeled with different fluorescent dyes allowing the authors to*  
328 *visualize numerous (here they show 6) different labels in the same sample using spectral*  
329 *unmixing confocal microscopy. Serial section EM images of the same samples were then*  
330 *reconstructed and aligned with the fluorescence images to achieve correlated*  
331 *fluorescence/ultrastructure. Overall the data were compelling, with many beautiful examples of*  
332 *correlated fluorescence localization with 3D ultrastructure, nicely demonstrating the power of the*  
333 *technique. While the manuscript primarily focuses on tool development and offers little in the*  
334 *way of novel biological insight, I feel the potential future impact of the technique (i.e. ability to*  
335 *assign neural identities to volumetric connectomics EM datasets, ultrastructural localization of*  
336 *channels, receptors, etc.) will have broad appeal. There are several specific points that deserve*  
337 *attention:*

338

339 *-Nowhere in the manuscript do the authors validate their labeling reagents in a knockout*  
340 *background. In many cases the labeling pattern is distinct, consistent with previously published*  
341 *work and the localization of the signal makes sense with the correlated ultrastructure (i.e.*  
342 *vGLUT labels presynaptic terminals), but in some cases it is more ambiguous. For example, in*  
343 *Fig. S2a,e the authors argue that the CB and PV scFvs label more of the target proteins in the*  
344 *cell nucleus, is this real signal or are these probes picking up something non-specific in the*  
345 *nucleus that the IgG does not?*

346 Concerning validation, we agree with the reviewer that the most crucial concern for  
347 immuno-probes or any similar affinity probes is whether they label or detect the actual target  
348 they are supposed to bind to. There are many cases when antibodies working in ELISA or  
349 Western blot settings fail to label their targets or have off-target labeling that creates abnormal  
350 background signals in immunohistochemistry (IHC). The parental (aka. progenitor) monoclonal  
351 antibodies (mAbs) from the UC Davis/NIH NeuroMab facility, whose sequences were used to  
352 generate the eight scFvs in this study, have undergone a strict validation process. In all but one  
353 case (the anti-NPY mAb), the mAbs have passed by at least three of the following:  
354 immunofluorescence on transfected COS-1 cells, Western blots on homogenized rat and mouse  
355 brains, IHC on rat and mouse brain sections, and IHC on mouse sections in a knockout  
356 background. These were accomplished in co-author James Trimmer's lab (for more details, see  
357 (Gong, Murray, and Trimmer 2016)). The validation tests of the eight mAbs used in the paper  
358 are now shown in new Supplementary Table 4). Although limited by the availability of KO brain  
359 samples, the three that we were able to test of them (N206Bb/9, GFAP R416WT; K28/43, PSD-  
360 95; K14/16, Kv 1.2) have passed the test of IHC on WT versus KO mouse brain sections, in that  
361 all detectable labeling observed in WT sections was eliminated in KO sections (all three also  
362 passed on WT/KO comparison by immunoblot) in a knockout background. While we want to test  
363 all the mAbs in a knockout background, but we hope the reviewer understands that it is

364 challenging to gather KO animals brain samples for all seven endogenous targets because  
 365 some may be lethal mutations.

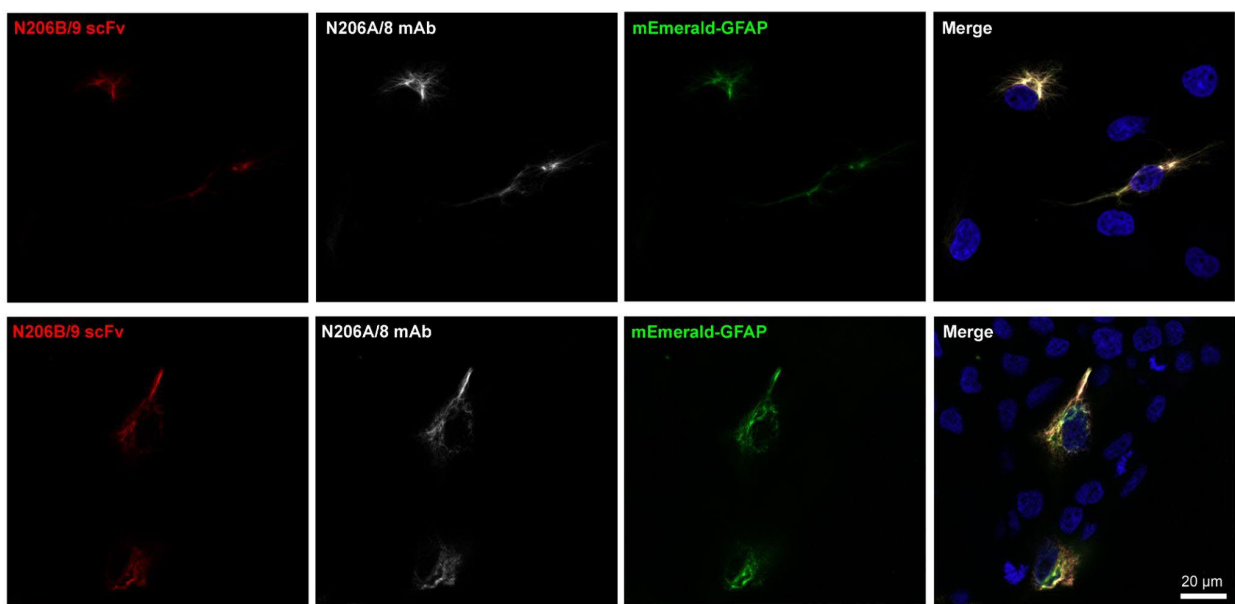
366 We also validated the scFvs in each case via IHC on rat and mouse brain sections and  
 367 by immunofluorescence immunocytochemistry on transiently transfected COS-1 cells (also  
 368 summarized in Supplementary Table 4; we also provide representative images in new  
 369 Supplementary Figure 9, 10, 11 for the validation of the N206b/9, anti-GFAP R416WT scFv.  
 370 Details of the methods of the validation tests for the other scFvs in this paper (and other scFvs)  
 371 can be found in (Mitchell et al. 2023; Gong, Murray, and Trimmer 2016). We have modified the  
 372 text to make these points clearer (line 139;line 143).

373

374 **Sup. Table 4. Information on the validation of the scFvs and their parental mAbs.**

Target	Clone No.	mAb validation				scFv validation
		COS-IF	Brain IB	Brain IHC	KO Brain IHC	Method
GFP	N86/38	Pass	NA	NA	NA	COS-IF
Calbindin	L109/57	Pass	Pass	Pass	ND	Brain IHC and COS-IF
GFAP R416WT	N206B/9	Pass	Pass	Pass	Pass	Brain IHC and COS-IF
VGluT1	N28/9	Pass	Pass	Pass	ND	Brain IHC and COS-IF
PSD-95	K28/43	Pass	Pass	Pass	Pass	Brain IHC and COS-IF
Kv 1.2	K14/16	Pass	Pass	Pass	Pass	Brain IHC and COS-IF
Parvalbumin	L114/81	Pass	Pass	Pass	ND	Brain IHC and COS-IF
NPY	L115/13	Pass	Fail	Pass	ND	COS-IF

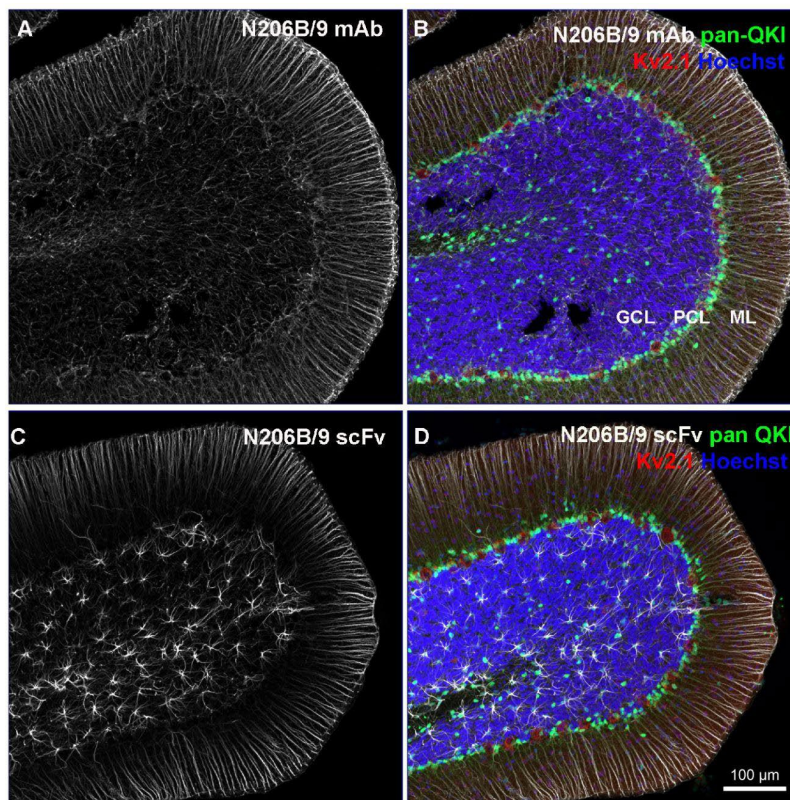
375



376 **Sup. Figure 9. Validation of anti-GFAP scFv with Immunofluorescence immunocytochemistry.**  
 377

378 Immunofluorescence immunocytochemistry on transiently transfected cells. COS-1 cells (top row) and  
 379 HEK293T cells (bottom row). Cells were transfected with a plasmid mEmerald-tagged human GFAP

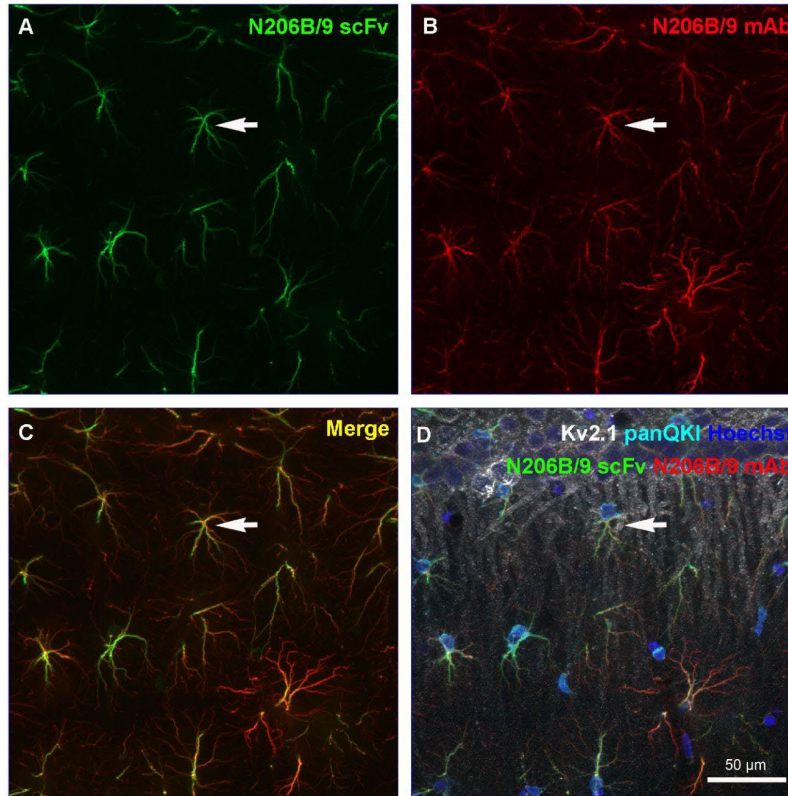
380 (green) and double immunolabeled with the 5-TAMRA-labeled anti-GFAP N206B/9 scFv (red) and the  
381 anti-GFAP N206A/8 mouse IgG1 mAb (white). Hoechst nuclear labeling is shown in blue.  
382  
383



384  
385 **Sup. Figure 10. Validation of anti-GFAP scFv with Immunofluorescence immunohistochemistry**  
386 **(cerebellum).**

387 GFAP scFv and original monoclonal antibody from which it was derived display the same tissue labeling  
388 pattern of a sagittal section through the rat cerebellum. **A)** Glial cells throughout the cerebellar granule  
389 cell layer (GCL) and prominent Bergmann glial process in molecular layer (ML) are labeled with  
390 hybridoma derived monoclonal antibody N206B/9. **B)** merged image includes labeling with a polyclonal  
391 rabbit antibody (KC) against the neuronal potassium channel Kv2.1, monoclonal antibody targeting glial  
392 specific RNA binding protein QKI (N147/6) and nuclear specific Hoechst labeling. **C)** An adjacent section  
393 labeled with N206B/9 derived scFv shows the same pattern of labeling. **D)** merged image with the same  
394 additional labeling as B.

395



396

397 **Sup. Figure 11. Validation of anti-GFAP scFv with Immunofluorescence immunohistochemistry**  
 398 **(hippocampus).**

399 Validation of scFv labeling pattern against hybridoma-generated monoclonal antibody N206B/9 from  
 400 which it was derived. Multiplex immunofluorescent labeling of a sagittal section through rat hippocampal  
 401 region CA1. **A)** 5-TAMRA conjugated N206B/9 derived scFv, **B)** Hybridoma derived monoclonal antibody  
 402 N206B/9 indirectly labeled with Alexa fluor 647 conjugated goat anti-mouse IgG1 secondary antibody, **C)**  
 403 merged images from A and B illustrating co-labeled astroglial cells (e.g arrowheads). **D)** Same multiplex  
 404 image shown in C with additional neuronal specific potassium channel Kv2.1, glial specific pan-QKI RNA  
 405 binding protein, and DNA marker Hoechst 33342 labeling.

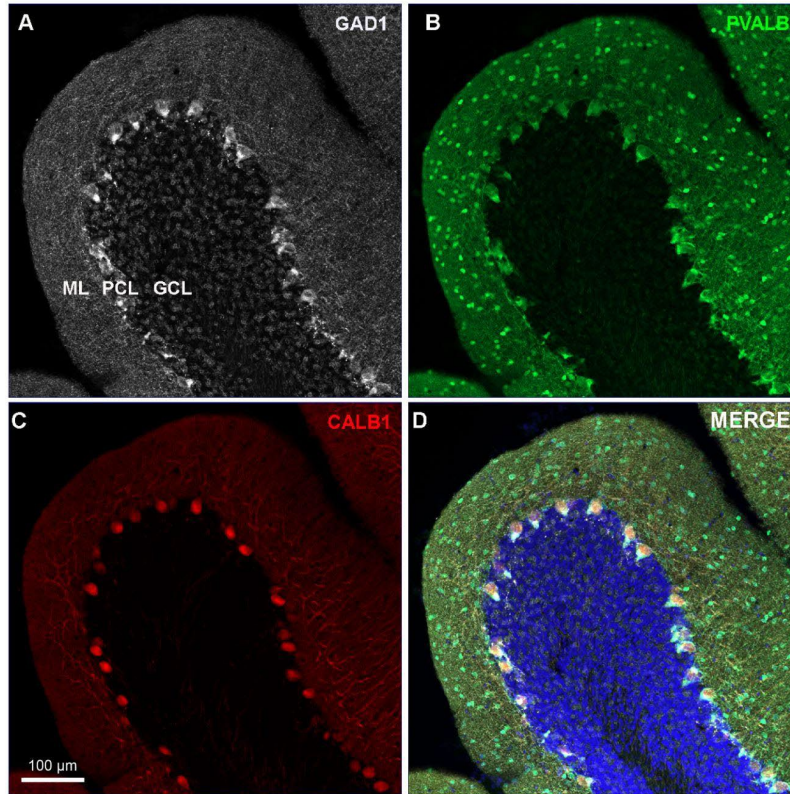
406

407 The second issue raised is concern over the ambiguous signals detected by the anti-  
 408 calbindin and anti-parvalbumin scFvs in the cell nuclei of Purkinje cells. Clearly, in the original  
 409 Supplementary Figure 2, the mAbs for calbindin and parvalbumin did not detect signals in the  
 410 cell nuclei as the scFvs did. In the revised paper we now include the validation IHC images of  
 411 the anti-calbindin and anti-parvalbumin mAbs from experiments done in James Trimmer's lab  
 412 (new Supplementary Figure 14). These images showed the normal expected labeling, that  
 413 included signal in some cell nuclei of Purkinje cells in the lateral hemisphere of the rat  
 414 cerebellum. In the original manuscript, we mentioned previous studies reporting the detection of  
 415 calbindin and parvalbumin in cell nuclei of Purkinje cells (Celio 1990; Brandenburg et al. 2021;  
 416 German et al. 1997; Schmidt et al. 2007). We believe calbindin and parvalbumin are present in  
 417 the cell nuclei. We therefore suspect that the reason our mAb labeling didn't detect signals in  
 418 the cell nuclei is insufficient antibody incubation time.

419 To address this problem, in Triton-X-treated samples, we first did immunolabeling with  
420 the same anti-calbindin and anti-parvalbumin mAbs directly conjugated with the red fluorophore  
421 FL-550 in distinction to using secondary antibodies as we did previously. The directly  
422 conjugated mAbs exclude the requirement for secondary antibodies allowing for only one round  
423 of incubation. We extended the incubation time to seven days (versus 2 days of incubation with  
424 primary antibodies previously). The results showed that both mAbs can detect signals in the cell  
425 nuclei of most (>~90%) Purkinje cells (new Supplementary Figure 15 c, l). This staining is  
426 similar to the scFv labeling except that scFvs were detected in all Purkinje cells. The second  
427 approach we attempted was immunolabeling with commercial polyclonal antibodies (pAbs)  
428 against calbindin and parvalbumin. These antibodies are not directly conjugated with  
429 fluorophores, so we utilized (Fab)<sub>2</sub> as fluorescently tagged secondaries, which are smaller than  
430 conventional secondaries and supposedly can diffuse in tissue better. Our results showed that,  
431 again, both calbindin and parvalbumin could be detected by the pAbs in the cell nuclei in most  
432 but not all Purkinje cells (new Supplementary Figure 15 d and m). The third approach we used,  
433 was to slice the section in a different orientation to cut through the nuclei of most Purkinje cells  
434 in order to gain direct access to the nuclei in the vibratome section (see new Supplementary  
435 Figure 15 e). We immunolabeled with the same anti-calbindin or anti-parvalbumin mAbs directly  
436 conjugated with the fluorophore FL-550 with a seven-day incubation. This time, we observed  
437 labeling in nearly all Purkinje cells (Supplementary Figure 15 f and n). These results indicate  
438 that the signals detected in the cell nuclei by scFvs are real signals. The reason it is relatively  
439 harder for full-length antibodies (mAbs or pAb) to detect these signals can be attributed to their  
440 relatively weaker penetration ability, even in the presence of Triton-X. This can be addressed in  
441 ways like extending incubation time or slicing sections to expose the internal epitopes in cell  
442 nuclei better. We have modified the text to make these points clearer (line 148).

443





444

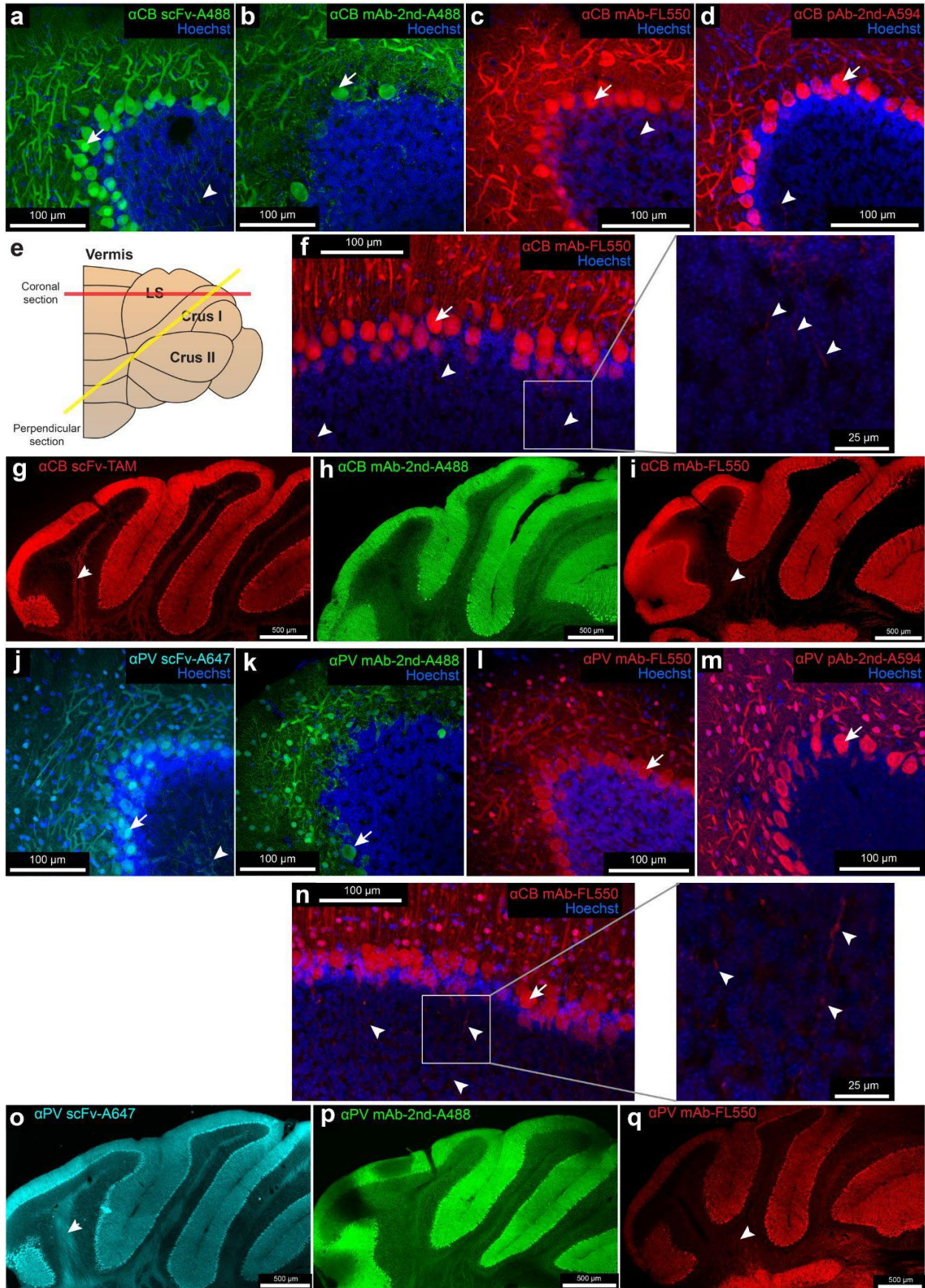
445 **Sup. Figure 14. Validation of anti-calbindin and anti-parvalbumin scFvs with Immunofluorescence**  
 446 **immunohistochemistry.**

447 Labeling pattern of original mAbs used to generate scFvs against Parvalbumin and Calbindin in rat  
 448 cerebellum. Sagittal section through cerebellum labeled with monoclonal antibodies L127/8 (A, GAD1),  
 449 L114/8 R (B, PARV), and L109/57 (C, CALB1). The merged image (D) shows the colocalized pattern of  
 450 labeling within Purkinje cell layer (PCL). ML, molecular layer, GCL, granule cell layer.

451

452





454 **Sup. Figure 15. Validation of immunofluorescence by scFv probes and their parental mAbs (part**  
455 **3).**

456 Cerebellum Crus 1 sections were immunolabeled with a calbindin-specific scFv (a), or its parental mAb  
457 and secondary antibody conjugated with Alexa Fluor 488 (b), the mAb conjugated with FL550 (c), or a  
458 commercial calbindin-specific pAb and secondary (Fab)<sub>2</sub> conjugated with Alexa Fluor 594 (d). e,  
459 Schematics showing the cutting orientation that is parallel to the lobule of Crus 1, which intersects  
460 perpendicular to the planer Purkinje cells in Crus 1. f, Sections cut in this orientation immunolabeled with  
461 the mAb conjugated with FL550. The boxed inset is shown enlarged in the adjacent panel. Whole-section  
462 images of cerebellum Crus 1 sections immunolabeled with a calbindin-specific scFv (g), or its parental  
463 mAb and secondary antibody conjugated with Alexa Fluor 488 (h), or the mAb conjugated with FL550 (i).  
464 Arrows indicate labeled cell nuclei of Purkinje cells. Arrowheads indicate the labeled axons.

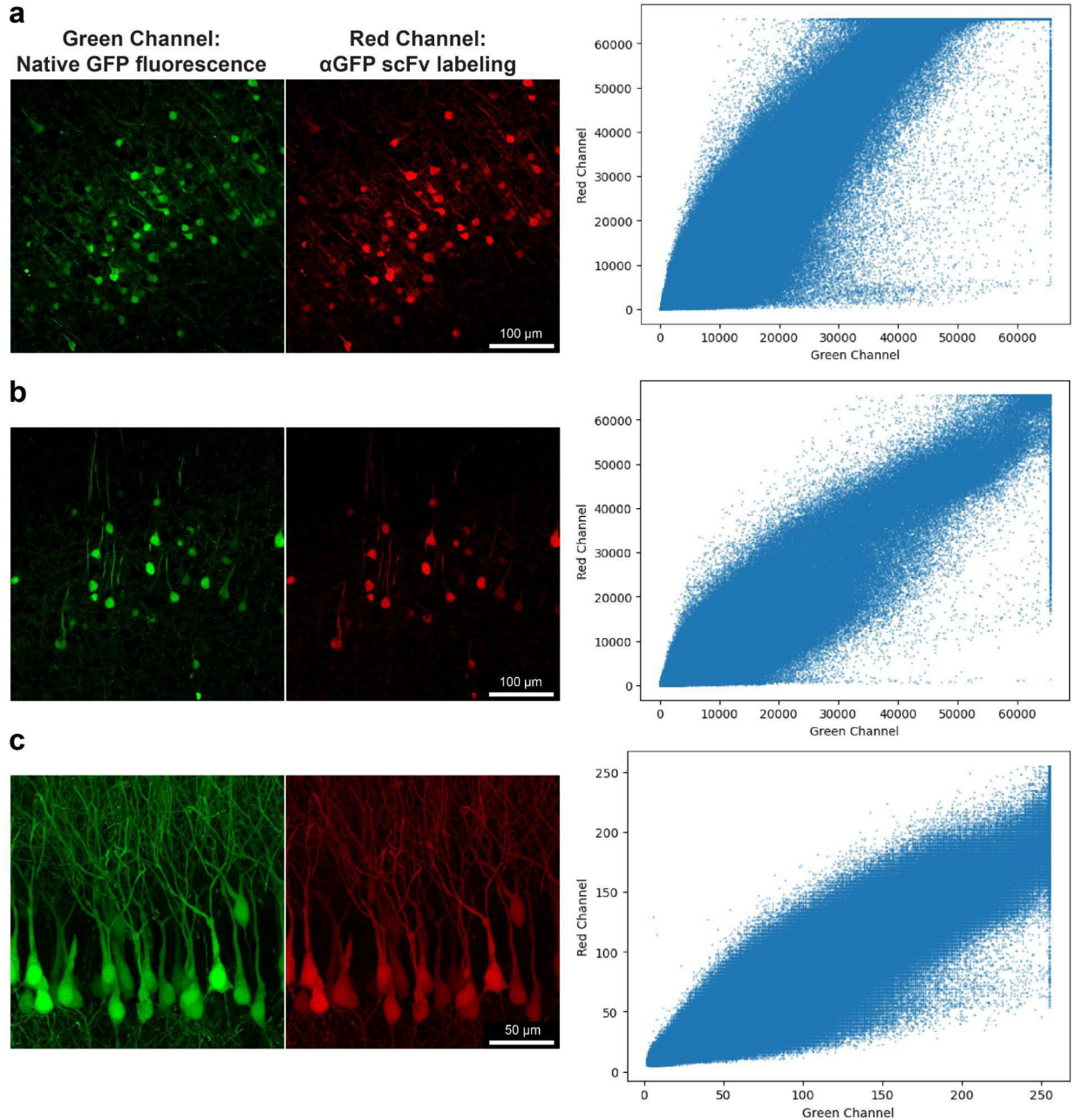
465  
466 Cerebellum Crus 1 sections were immunolabeled with a parvalbumin-specific scFv (j), or its parental mAb  
467 and secondary antibody conjugated with Alexa Fluor 488 (k), the mAb conjugated with FL550 (l), or a  
468 commercial parvalbumin-specific pAb and secondary (Fab)<sub>2</sub> conjugated with Alexa Fluor 594 (m). f,  
469 Sections cut in this orientation in e immunolabeled with the mAb conjugated with FL550. The boxed inset  
470 is shown enlarged in the adjacent panel. Whole-section images of cerebellum Crus 1 sections  
471 immunolabeled with a parvalbumin-specific scFv (o), or its parental mAb and secondary antibody  
472 conjugated with Alexa Fluor 488 (p), or the mAb conjugated with FL550 (q). Arrows indicate labeled cell  
473 nuclei of Purkinje cells. Arrowheads indicate the labeled axons.

474  
475 *-While many of the images are quite striking, overall the manuscript lacked any sort of*  
476 *quantitative analysis. Just as one example, in Fig. 1, showing a simple pixel correlation scatter*  
477 *plot comparing the YFP and GFP-scFv signal would give readers a better idea of how evenly*  
478 *the scFv is penetrating cells to label YFP.*

479 We thank the reviewer for highlighting the lack of quantitative analysis in comparing the  
480 specificity of scFvs and mAbs. The paper does contain other quantitative analyses (see Figure  
481 7; Supplementary Figure 29; Supplementary Table 5, 6) but in response to the specific question  
482 raised, we have now created pixel correlation scatter plots for three images from two cortical  
483 and one hippocampal section from YFP-H mice, which were also immunolabeled with the anti-  
484 GFP scFv (new Supplementary Figure 2). Supplementary Figure 2 a is the raw image of Figure  
485 1 b. As is shown in all three pixel correlating scatter plots, the signals from the scFv labeling  
486 (red) correlate with the native YFP fluorescence signal (green). There are pixels that only have  
487 values in the green channels, which correspond to the insufficiently labeled axons pointed out in  
488 Figure 2 a. There are very few pixels that only have values in the red (scFv) channel, which  
489 indicates that there is minimal off-target labeling of this anti-GFP scFv. This analysis gives us  
490 confidence in the specificity of the scFv for green fluorescent protein. Doing this kind of double  
491 labeling is more problematic when comparing scFvs to mAbs that have the identical paratope as  
492 they compete for the same site. So, in these cases, as described in detail above, we had to be  
493 content with the comparative labeling of different tissue sections. We have modified the text to  
494 make this point clearer (line 128).

495





496  
497  
498

**Sup. Figure 2. Pixel correlation scatter plots comparing the native YFP fluorescence signal and the red fluorescence from the labeling of the GFP- specific scFv.**

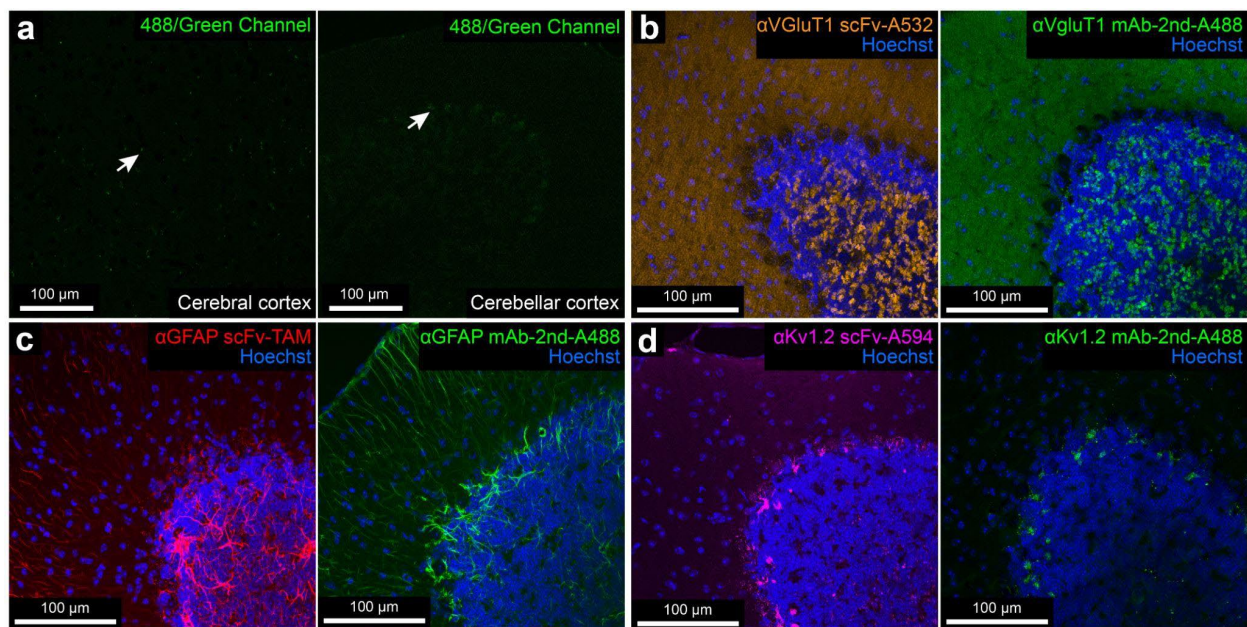
499 Cerebral cortex samples (**a** and **b**) and hippocampus (**c**) from YFP-H mice were immunolabeled with a  
500 GFP-specific scFv conjugated with the red fluorophore 5-TAMRA. The images are raw data without any  
501 brightness/contrast adjustment. **a** is the raw image data of Figure 1 b.  
502

503 *-p. 9 ".....immunofluorescence patterns that were similar to or in some cases stronger than their*  
504 *parental mAbs in Crus 1 of the cerebellar cortex (Figure 2 a; Sup. Figure 2; Sup. Figure 3). In*  
505 *many cases the comparisons between mAb and scFv is not entirely fair since the mAb is*  
506 *labeled in the 488/green channel (in which brain tissue notoriously has more autofluorescence)*  
507 *and the scFv in the red channel e.g. NPY signal in Sup. 2b,d; PSD95 in Sup. 2f. Is the labeling*

508 *really that much cleaner or is the background signal in the green channel making the mAb*  
509 *appear worse than it is?*

510 We apologize that the phrasing in our original manuscript may have caused a  
511 misunderstanding. In this sentence, “in some cases stronger than their parental mAbs in Crus 1  
512 of the cerebellar cortex.” only refers to the cases of calbindin and parvalbumin, as discussed in  
513 the previous point. In the other cases (GFAP, VGluT1, Kv 1.2, PSD-95, and NPY), we believe  
514 our results suggest that the labeling of scFvs and mAbs are comparably good in terms of both  
515 signal and background. We understand the legitimate concern that the tissue sections fixed with  
516 formaldehyde and glutaraldehyde may have a higher background in the 488/green channel.  
517 Glutaraldehyde especially has stronger autofluorescence (Fischer et al. 2008). However, we  
518 only used 0.1% glutaraldehyde in our preparation prior to osmium staining. After adequate  
519 washing with PBS, the brain tissue sections do not show strong autofluorescence in the  
520 488/green channel (as now shown in new Supplementary Figure 12 a). There is some  
521 autofluorescence, mostly from lipofuscin granules in cell bodies (arrows in new Supplementary  
522 Figure 12 a) with broad excitation/emission spectra (Di Guardo 2015; Marmorstein et al. 2002).  
523 But this autofluorescence is found in all channels. We emphasize that we are not attempting to  
524 make a case that scFv labeling is cleaner than that obtained with mAb, as the results from both  
525 are very similar. Indeed we also performed new experiments with red fluorophore-conjugated  
526 mAbs for calbindin and parvalbumin, as discussed in our answer to the reviewer’s point 1, and  
527 didn’t find any difference in the background level (new Supplementary Figure 15). We have  
528 adjusted the phrasing in the manuscript (line 145) to avoid any further misunderstanding.

529



530  
531  
532  
533

**Sup. Figure 12. Validation of immunofluorescence by scFv probes and their parental mAbs (part 1).**

534 **a**, Confocal images from unlabeled the cerebral cortex and cerebellar cortex of a wild-type mouse  
535 showed limited background in the 488/green channel. Arrows indicate background signals lipofuscin  
536 granule. **b-d**, Cerebellum Crus 1 sections were immunolabeled with scFvs targeting VGluT1, GFAP, and

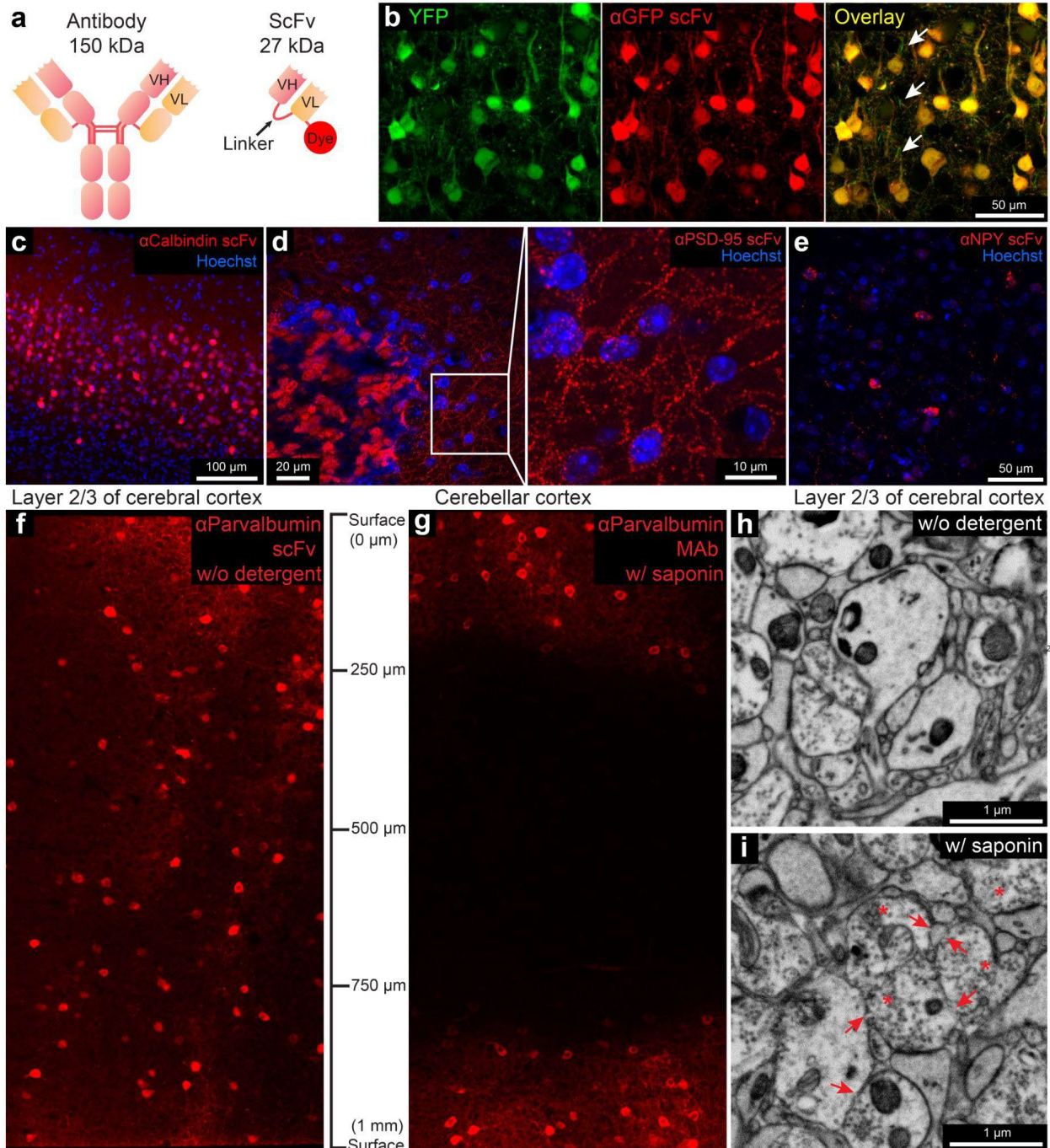
537 Kv 1.2; or these scFvs' parental mAbs and secondary antibodies conjugated with Alexa Fluor 488.  
538  
539

540 *-p. 9 ".....found that the anti-calbindin scFv penetrated to a depth of ~150 μm in a 300-μm tissue*  
541 *slice". So the probe labeled throughout the entire slice?*

542 We apologize for the lack of clarity, yes, we meant that they labeled through the entire  
543 300 μm slice (150 μm from each side). Given the recent availability of directly conjugated mAbs  
544 we have removed Figure 1 d and e to Supplementary Figure 3 b (we remade figures from raw  
545 images showing the penetration across the 300 μm thickness) and c, and added new Figure 1 f-  
546 i, Supplementary Figure 4 and 5 of the results of a comparable experiment of scFv labeling on  
547 300-μm and 1-mm thick brain tissue sections in the absence of detergent. In Figure 1 and  
548 Supplementary Figure 4, scFvs are shown to label throughout a 1-mm thickness with a seven-  
549 day incubation; in Supplementary Figure 5, scFvs can label a 300-μm thickness sample with  
550 either a 1- or 3-day incubation. EM ultrastructure of all these samples was good. We have  
551 modified the text to make these points clearer (line 150).

552





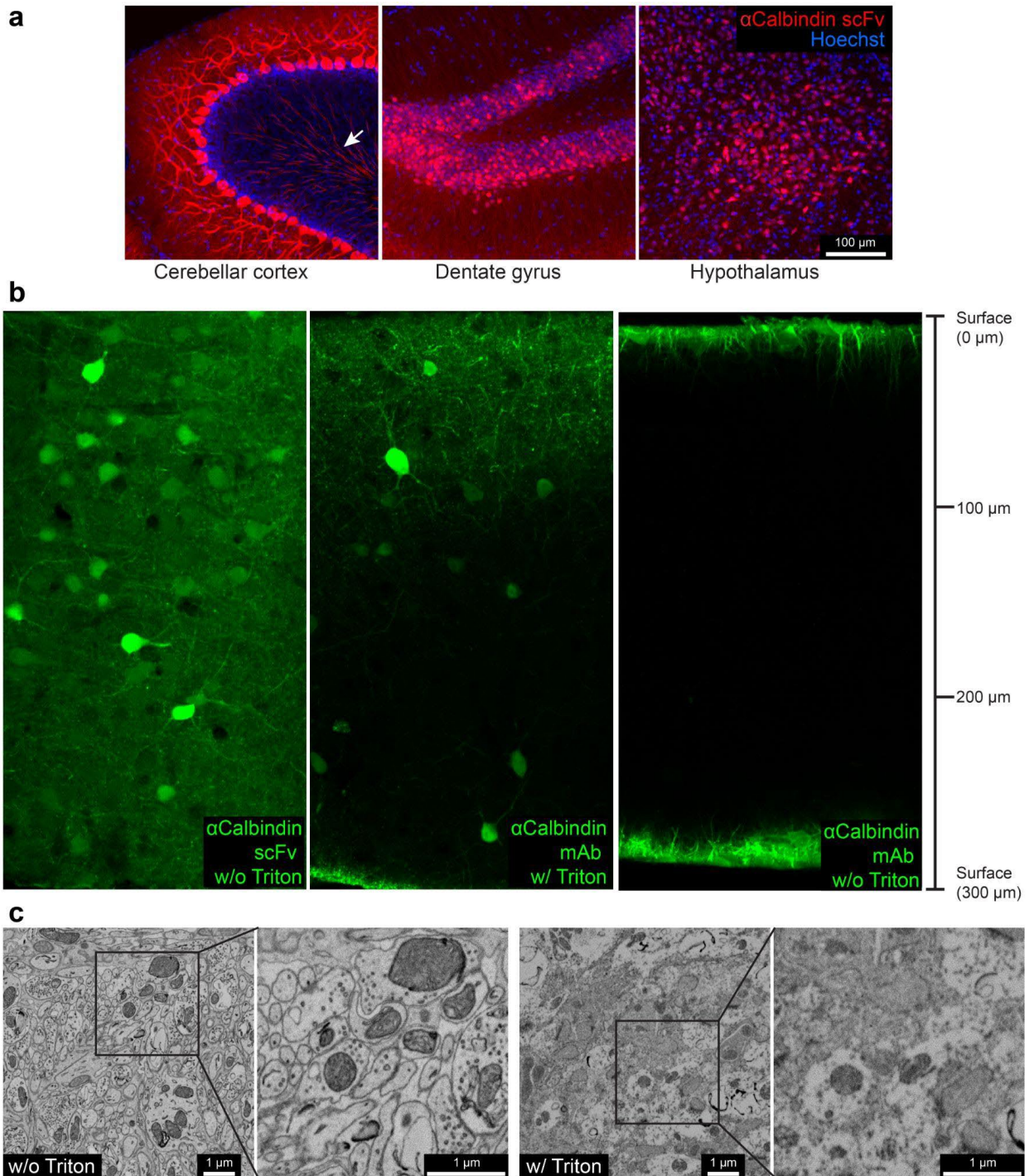
553

554 **Figure 1. Fluorescent scFv probes label brain tissues without detergents to preserve electron**  
 555 **microscopy ultrastructure.**

556 **a**, Schematic representations of a full-length IgG antibody and an scFv probe with a conjugated  
 557 fluorescent dye. **b**, Confocal images from the cerebral cortex of a YFP-H mouse labeled using a GFP-  
 558 specific scFv probe conjugated with the red dye 5-TAMRA. Arrows show thinner neuronal processes,  
 559 perhaps myelinated, that are not labeled by scFv. **c**, Layer 2/3 of the cerebral cortex labeled with a  
 560 calbindin-specific scFv probe. **d**, Cerebellum cortex of Crus 1 labeled with the PSD-95 specific scFv. Right  
 561 panel is the enlarged boxed inset from left. **e**, Cerebral cortex labeled with the NPY-specific scFv. **f** and **g**,  
 562 Tissue penetration comparison of a parvalbumin-specific scFv without detergent and its parental



563 mAbs directly conjugated with fluorophores with 0.05% saponin on 1-mm cerebral cortex tissue sections  
 564 with a 7-day incubation. **h** and **i**, Comparison of ultrastructure from samples incubated 7 days without  
 565 detergent and with 0.05% saponin. Arrows indicate membrane breaks. Asterisks indicate abnormal  
 566 appearing vesicle-filled axonal terminals.  
 567

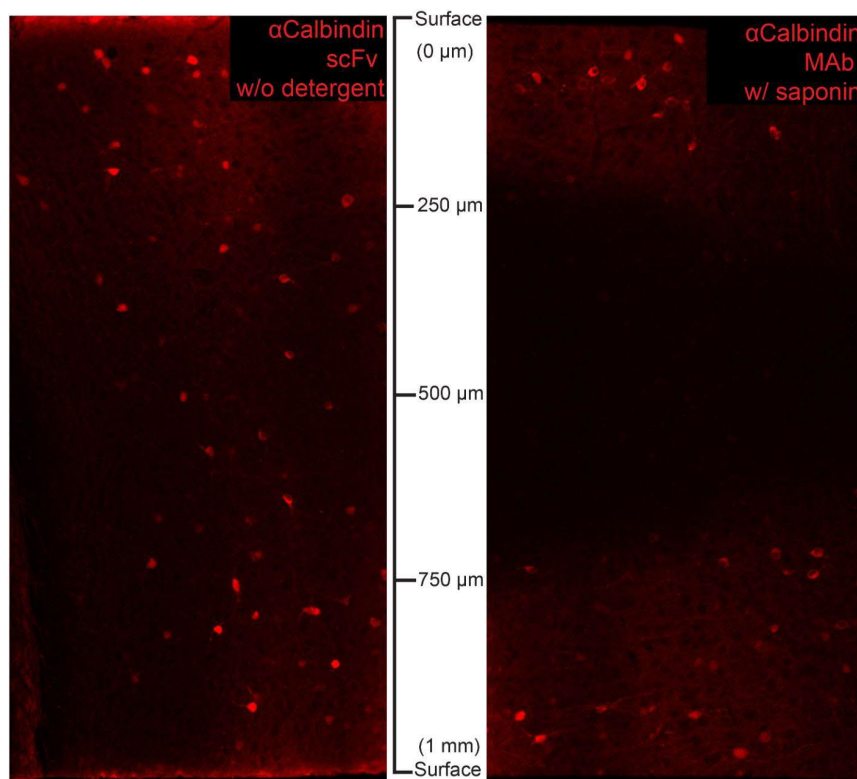


568 **Sup. Figure 3. Immunolabeling results of anti-calbindin scFv and tissue penetration comparison.**  
 569

570 **a**, Additional brain regions labeled with a calbindin-specific scFv probe conjugated with 5-TAMRA. The  
 571 arrow in the left panel shows myelinated Purkinje cell axons in the granule layer. **b**, Tissue penetration



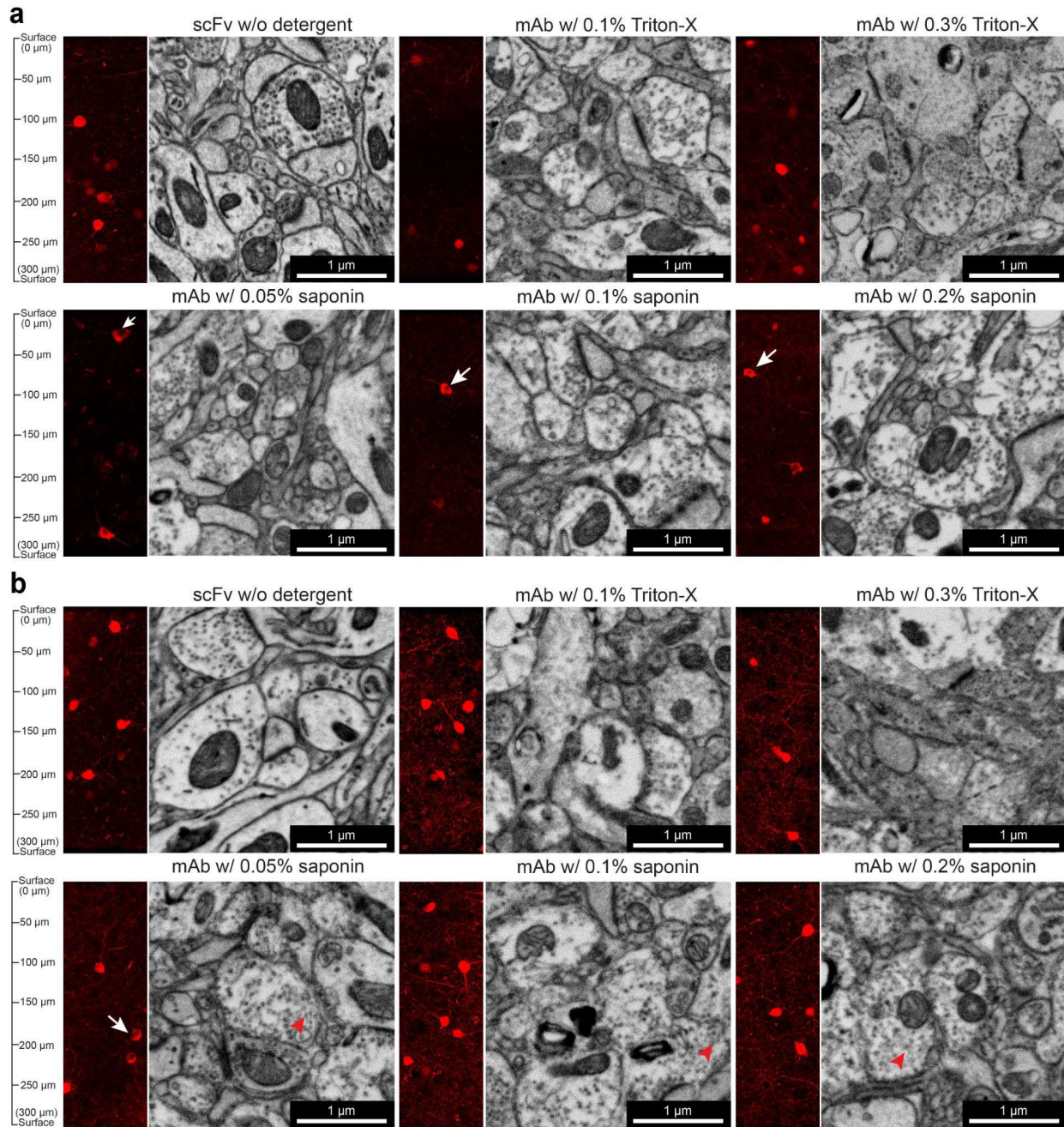
572 depth comparison of scFvs, mAbs (plus secondary antibodies), and the role of detergents in improving  
573 the depth of labeling. **c**, Comparison of ultrastructure with and without 0.5% Triton X-100 on scFv labeled  
574 samples. Boxed insets are shown at higher magnification in adjacent panels. of ~30  $\mu\text{m}$ ; the nanobody  
575 can penetrate into a depth of ~150  $\mu\text{m}$ .  
576



577  
578  
579

**Sup. Figure 4. Penetration of anti-calbindin scFv into 1-mm tissue sample.**

580 Tissue penetration depth comparison of a calbindin-specific scFv without detergent and its parental mAbs  
581 directly conjugated with fluorophores with 0.05% saponin on 1-mm cerebral cortex tissue sections with a  
582 7-day incubation.  
583  
584



585  
586  
587  
588

**Sup. Figure 5. Tissue penetration depth comparison of scFvs in the absence of detergent and fluorophore-conjugated mAbs with the treatments of various concentrations of detergents.**

589 300- $\mu\text{m}$  cerebral cortex sections were immunolabeled for one day (a) or seven days (b) with a calbindin-  
590 specific scFv conjugated with 5-TAMRA in the absence of detergent or with the scFv's parental mAb  
591 conjugated with FL550 in the presence of 0.1%, 0.3% Triton-X, or 0.05%, 0.1%, 0.2% saponin. Arrows  
592 indicate unlabeled cell nuclei. Arrowheads indicate granular textures associated with the treatment of  
593 saponin.

594

595

596 **References**

- 597 Ahmad, Zuhaida Asra, Swee Keong Yeap, Abdul Manaf Ali, Wan Yong Ho, Noorjahan Banu  
598 Mohamed Alitheen, and Muhajir Hamid. 2012. "scFv Antibody: Principles and Clinical  
599 Application." *Clinical & Developmental Immunology* 2012 (March): 980250.
- 600 Alric, Christophe, Katel Hervé-Aubert, Nicolas Aubrey, Souad Melouk, Laurie Lajoie, William  
601 Mème, Sandra Mème, et al. 2018. "Targeting HER2-Breast Tumors with scFv-Decorated  
602 Bimodal Nanoprobos." *Journal of Nanobiotechnology* 16 (1): 18.
- 603 Beer, Marit A. de, and Ben N. G. Giepmans. 2020. "Nanobody-Based Probes for Subcellular  
604 Protein Identification and Visualization." *Frontiers in Cellular Neuroscience* 14 (November):  
605 573278.
- 606 Bernard, Clémence, Clémentine Vincent, Damien Testa, Eva Bertini, Jérôme Ribot, Ariel A. Di  
607 Nardo, Michel Volovitch, and Alain Prochiantz. 2016. "A Mouse Model for Conditional  
608 Secretion of Specific Single-Chain Antibodies Provides Genetic Evidence for Regulation of  
609 Cortical Plasticity by a Non-Cell Autonomous Homeoprotein Transcription Factor." *PLoS*  
610 *Genetics* 12 (5): e1006035.
- 611 Bird, R. E., K. D. Hardman, J. W. Jacobson, S. Johnson, B. M. Kaufman, S. M. Lee, T. Lee, S.  
612 H. Pope, G. S. Riordan, and M. Whitlow. 1988. "Single-Chain Antigen-Binding Proteins."  
613 *Science* 242 (4877): 423–26.
- 614 Blanc, Hugo, Gabriel Kaddour, Nicolas B. David, Willy Supatto, Jean Livet, Emmanuel  
615 Beaurepaire, and Pierre Mahou. 2023. "Chromatically Corrected Multicolor Multiphoton  
616 Microscopy." *ACS Photonics* 10 (12): 4104–11.
- 617 Brandenburg, Cheryl, Lindsey A. Smith, Michaela B. C. Kilander, Morgan S. Bridi, Yu-Chih Lin,  
618 Shiyong Huang, and Gene J. Blatt. 2021. "Parvalbumin Subtypes of Cerebellar Purkinje  
619 Cells Contribute to Differential Intrinsic Firing Properties." *Molecular and Cellular*  
620 *Neurosciences* 115 (September): 103650.
- 621 Celio, M. R. 1990. "Calbindin D-28k and Parvalbumin in the Rat Nervous System."  
622 *Neuroscience* 35 (2): 375–475.
- 623 Cheng, Ruoyu, Feng Zhang, Meng Li, Xiang Wo, Yu-Wen Su, and Wei Wang. 2019. "Influence  
624 of Fixation and Permeabilization on the Mass Density of Single Cells: A Surface Plasmon  
625 Resonance Imaging Study." *Frontiers in Chemistry* 7 (August): 588.
- 626 Di Guardo, G. 2015. "Lipofuscin, Lipofuscin-like Pigments and Autofluorescence." *European*  
627 *Journal of Histochemistry: EJH* 59 (1): 2485.
- 628 Fischer, Andrew H., Kenneth A. Jacobson, Jack Rose, and Rolf Zeller. 2008. "Fixation and  
629 Permeabilization of Cells and Tissues." *CSH Protocols* 2008 (May): db.top36.
- 630 Fox, C. H., F. B. Johnson, J. Whiting, and P. P. Roller. 1985. "Formaldehyde Fixation." *The*  
631 *Journal of Histochemistry and Cytochemistry: Official Journal of the Histochemistry Society*  
632 33 (8): 845–53.
- 633 Franek, Michal, Lenka Koptašíková, Jíří Mikšátko, David Liebl, Eliška Macíčková, Jakub  
634 Pospíšil, Milan Esner, Martina Dvořáčková, and Jíří Fajkus. 2024. "In-Section Click-iT  
635 Detection and Super-Resolution CLEM Analysis of Nucleolar Ultrastructure and Replication  
636 in Plants." *Nature Communications* 15 (1): 2445.
- 637 Fulton, Kara A., and Kevin L. Briggman. 2021. "Permeabilization-Free En Bloc  
638 Immunohistochemistry for Correlative Microscopy." *eLife* 10 (May).  
639 <https://doi.org/10.7554/eLife.63392>.
- 640 Furuta, Takahiro, Kenta Yamauchi, Shinichiro Okamoto, Megumu Takahashi, Soichiro Kakuta,  
641 Yoko Ishida, Aya Takenaka, et al. 2022. "Multi-Scale Light Microscopy/electron Microscopy  
642 Neuronal Imaging from Brain to Synapse with a Tissue Clearing Method, ScaleSF."  
643 *iScience* 25 (1): 103601.
- 644 German, D. C., M. C. Ng, C. L. Liang, A. McMahon, and A. M. Iacopino. 1997. "Calbindin-D28k  
645 in Nerve Cell Nuclei." *Neuroscience* 81 (3): 735–43.

646 Gong, Belvin, Karl D. Murray, and James S. Trimmer. 2016. "Developing High-Quality Mouse  
647 Monoclonal Antibodies for Neuroscience Research - Approaches, Perspectives and  
648 Opportunities." *New Biotechnology* 33 (5 Pt A): 551–64.

649 Huston, J. S., D. Levinson, M. Mudgett-Hunter, M. S. Tai, J. Novotný, M. N. Margolies, R. J.  
650 Ridge, R. E. Brucoleri, E. Haber, and R. Crea. 1988. "Protein Engineering of Antibody  
651 Binding Sites: Recovery of Specific Activity in an Anti-Digoxin Single-Chain Fv Analogue  
652 Produced in *Escherichia Coli*." *Proceedings of the National Academy of Sciences of the  
653 United States of America* 85 (16): 5879–83.

654 Ichikawa, Takehiko, Dong Wang, Keisuke Miyazawa, Kazuki Miyata, Masanobu Oshima, and  
655 Takeshi Fukuma. 2022. "Chemical Fixation Creates Nanoscale Clusters on the Cell Surface  
656 by Aggregating Membrane Proteins." *Communications Biology* 5 (1): 487.

657 Im, Sun-Woo, Hee Yong Chung, and Young-Ju Jang. 2017. "Development of Single-Chain Fv of  
658 Antibody to DNA as Intracellular Delivery Vehicle." *Animal Cells and Systems* 21 (6): 382–  
659 87.

660 Januszewski, Michał, Jürgen Kornfeld, Peter H. Li, Art Pope, Tim Blakely, Larry Lindsey,  
661 Jeremy Maitin-Shepard, Mike Tyka, Winfried Denk, and Viren Jain. 2018. "High-Precision  
662 Automated Reconstruction of Neurons with Flood-Filling Networks." *Nature Methods* 15 (8):  
663 605–10.

664 Kiernan, John A. 2000. "Formaldehyde, Formalin, Paraformaldehyde And Glutaraldehyde: What  
665 They Are And What They Do." *Microscopy Today* 8 (1): 8–13.

666 Kim, Eunhee G., Jieun Jeong, Junghyeon Lee, Hyeryeon Jung, Minho Kim, Yi Zhao, Eugene C.  
667 Yi, and Kristine M. Kim. 2020. "Rapid Evaluation of Antibody Fragment Endocytosis for  
668 Antibody Fragment-Drug Conjugates." *Biomolecules* 10 (6).  
669 <https://doi.org/10.3390/biom10060955>.

670 Li, Tengfei, Matthias Vandesquille, Fani Koukoulis, Clémence Duffeffant, Ihsen Youssef, Pascal  
671 Lenormand, Christelle Ganneau, et al. 2016. "Camelid Single-Domain Antibodies: A  
672 Versatile Tool for in Vivo Imaging of Extracellular and Intracellular Brain Targets." *Journal of  
673 Controlled Release: Official Journal of the Controlled Release Society* 243 (December): 1–  
674 10.

675 Lu, Xiaotang, Xiaomeng Han, Yaron Meirovitch, Evelina Sjöstedt, Richard L. Schalek, and Jeff  
676 W. Lichtman. 2023. "Preserving Extracellular Space for High-Quality Optical and  
677 Ultrastructural Studies of Whole Mammalian Brains." *Cell Reports Methods* 3 (7): 100520.

678 Mahou, Pierre, Maxwell Zimmerley, Karine Loulier, Katherine S. Matho, Guillaume Labroille,  
679 Xavier Morin, Willy Supatto, Jean Livet, Delphine Débarre, and Emmanuel Beaurepaire.  
680 2012. "Multicolor Two-Photon Tissue Imaging by Wavelength Mixing." *Nature Methods* 9  
681 (8): 815–18.

682 Marmorstein, Alan D., Lihua Y. Marmorstein, Hirokazu Sakaguchi, and Joe G. Hollyfield. 2002.  
683 "Spectral Profiling of Autofluorescence Associated with Lipofuscin, Bruch's Membrane, and  
684 Sub-RPE Deposits in Normal and AMD Eyes." *Investigative Ophthalmology & Visual  
685 Science* 43 (7): 2435–41.

686 Mitchell, Keith G., Belvin Gong, Samuel S. Hunter, Diana Burkart-Waco, Clara E. Gavira-O'Neill,  
687 Kayla M. Templeton, Madeline E. Goethel, et al. 2023. "High-Volume Hybridoma  
688 Sequencing on the NeuroMabSeq Platform Enables Efficient Generation of Recombinant  
689 Monoclonal Antibodies and scFvs for Neuroscience Research." *Scientific Reports* 13 (1):  
690 16200.

691 Monnier, Philippe P., Robin J. Vigouroux, and Nardos G. Tassew. 2013. "In Vivo Applications of  
692 Single Chain Fv (Variable Domain) (scFv) Fragments." *Antibodies* 2 (2): 193–208.

693 Pudavar, Haridas, Judith Reddington, Jason A. Junge, Scott E. Fraser, and Giulia Ossato.  
694 2024. "STELLARIS 8 DIVE: A Rainbow of Possibilities with Multiphoton Excitation and  
695 Lifetime-Based Information." In *Multiphoton Microscopy in the Biomedical Sciences XXIV*,  
696 12847:32–33. SPIE.



- 697 Schmid, Benjamin, Gopi Shah, Nico Scherf, Michael Weber, Konstantin Thierbach, Citlali Pérez  
698 Campos, Ingo Roeder, Pia Aanstad, and Jan Huisken. 2013. "High-Speed Panoramic Light-  
699 Sheet Microscopy Reveals Global Endodermal Cell Dynamics." *Nature Communications* 4:  
700 2207.
- 701 Schmidt, Hartmut, Oliver Arendt, Edward B. Brown, Beat Schwaller, and Jens Eilers. 2007.  
702 "Parvalbumin Is Freely Mobile in Axons, Somata and Nuclei of Cerebellar Purkinje  
703 Neurons." *Journal of Neurochemistry* 100 (3): 727–35.
- 704 Shapson-Coe, Alexander, Michał Januszewski, Daniel R. Berger, Art Pope, Yuelong Wu, Tim  
705 Blakely, Richard L. Schalek, et al. 2021. "A Connectomic Study of a Petascale Fragment of  
706 Human Cerebral Cortex." *bioRxiv*. <https://doi.org/10.1101/2021.05.29.446289>.
- 707 Thavarajah, Rooban, Vidya Kazhiyur Mudimbaimannar, Joshua Elizabeth, Umadevi  
708 Krishnamohan Rao, and Kannan Ranganathan. 2012. "Chemical and Physical Basics of  
709 Routine Formaldehyde Fixation." *Journal of Oral and Maxillofacial Pathology: JOMFP* 16  
710 (3): 400–405.
- 711 Thiel, M. A., D. J. Coster, S. D. Standfield, H. M. Brereton, C. Mavrangelos, H. Zola, S. Taylor,  
712 A. Yusim, and K. A. Williams. 2002. "Penetration of Engineered Antibody Fragments into  
713 the Eye." *Clinical and Experimental Immunology* 128 (1): 67–74.
- 714 Tsuruel, Shlomo, Sagi Gudes, Ryan W. Draft, Alexander M. Binshtok, and Jeff W. Lichtman.  
715 2015. "Multispectral Labeling Technique to Map Many Neighboring Axonal Projections in  
716 the Same Tissue." *Nature Methods* 12 (6): 547–52.
- 717 Weisser, Nina E., and J. Christopher Hall. 2009. "Applications of Single-Chain Variable  
718 Fragment Antibodies in Therapeutics and Diagnostics." *Biotechnology Advances* 27 (4):  
719 502–20.
- 720 Wittrup, Anders, Si-He Zhang, Gerdy B. ten Dam, Toin H. van Kuppevelt, Per Bengtson, Maria  
721 Johansson, Johanna Welch, Matthias Mörgelin, and Mattias Belting. 2009. "ScFv Antibody-  
722 Induced Translocation of Cell-Surface Heparan Sulfate Proteoglycan to Endocytic  
723 Vesicles." *The Journal of Biological Chemistry* 284 (47): 32959–67.

## **REVIEWERS' COMMENTS**

Reviewer #1 (Remarks to the Author):

The authors have developed a method employing fluorescent single-chain variable fragments (scFvs) for conducting multiplexed detergent-free immunolabeling and volumetric-correlated-light-and-electron-microscopy (vCLEM) on the same samples. In this manuscript, they detail the development of eight fluorescent scFvs targeting specific markers crucial for brain studies. Through experimentation, six fluorescent probes were successfully visualized in the cerebellum using confocal microscopy with spectral unmixing, followed by vEM analysis of the identical sample. The outcomes reveal an exceptional blend of ultrastructure alongside multiple fluorescence channels, offering valuable insights into cellular composition and organization.

This approach facilitated the documentation of a previously poorly characterized cell type and the precise subcellular localization. Leveraging scFvs derived from existing monoclonal antibodies opens up the possibility of generating numerous such probes, which could significantly enhance molecular overlays for connectomic investigations.

This study represents a significant advancement in the field of vCLEM and holds great promise for researchers seeking to unravel intricate neuronal networks. The revised version of the manuscript effectively addresses key questions and concerns. I don't have further comments.

Reviewer #2 (Remarks to the Author):

The revised manuscript thoroughly addresses all of the concerns raised in my initial review. I think the manuscript will have broad appeal and I appreciate the effort put in to address the referees' comments. I strongly recommend publication in Nature Communications.

1 **REVIEWER COMMENTS**

2

3 **Reviewer #1 (Remarks to the Author):**

4 *The authors have developed a method employing fluorescent single-chain variable fragments*  
5 *(scFvs) for conducting multiplexed detergent-free immunolabeling and volumetric-correlated-*  
6 *light-and-electron-microscopy (vCLEM) on the same samples. In this manuscript, they detail the*  
7 *development of eight fluorescent scFvs targeting specific markers crucial for brain studies.*  
8 *Through experimentation, six fluorescent probes were successfully visualized in the cerebellum*  
9 *using confocal microscopy with spectral unmixing, followed by vEM analysis of the identical*  
10 *sample. The outcomes reveal an exceptional blend of ultrastructure alongside multiple*  
11 *fluorescence channels, offering valuable insights into cellular composition and organization.*

12

13 *This approach facilitated the documentation of a previously poorly characterized cell type and*  
14 *the precise subcellular localization. Leveraging scFvs derived from existing monoclonal*  
15 *antibodies opens up the possibility of generating numerous such probes, which could*  
16 *significantly enhance molecular overlays for connectomic investigations.*

17

18 *This study represents a significant advancement in the field of vCLEM and holds great promise*  
19 *for researchers seeking to unravel intricate neuronal networks. The revised version of the*  
20 *manuscript effectively addresses key questions and concerns. I don't have further comments.*

21 We thank the reviewer's comments. There's nothing to be further addressed.

22

23 **Reviewer #2 (Remarks to the Author):**

24 *The revised manuscript thoroughly addresses all of the concerns raised in my initial review. I*  
25 *think the manuscript will have broad appeal and I appreciate the effort put in to address the*  
26 *referees' comments. I strongly recommend publication in Nature Communications.*

27 We thank the reviewer's comments. There's nothing to be further addressed.

28

29

30